AERO. & ASTRO. LIBRARY

MASS. INST. TECH. DEC 8 1945 LIBRARY

AERO

NATIONAL ADVISORY COMMITTEE FOR AERONAUTICS

REPORT No. 748

copy #3

NORMAL-PRESSURE TESTS OF RECTANGULAR PLATES

By WALTER RAMBERG, ALBERT E. McPHERSON, and SAMUEL LEVY

1942

105

AERONAUTIC SYMBOLS

1. FUNDAMENTAL AND DERIVED UNITS

	Symbol	Metric		English	
		Unit	Abbreviation	Unit	Abbreviation
Length	l	meter	m	foot (or mile)	ft (or mi)
Time	t	second	s	second (or hour)	sec (or hr)
Force	F	weight of 1 kilogram	kg	weight of 1 pound	lb
Power	P	horsepower (metric)		horsepower	hp
Speed	V	kilometers per hour	kph	miles per hour	mph
		meters per second	mps	feet per second	fps

2. GENERAL SYMBOLS

W Weight $=mg$

g Standard acceleration of gravity $=9.80665$ m/s^2 or 32.1740 ft/sec^2

m Mass $=\frac{W}{g}$

I Moment of inertia $=mk^2$. (Indicate axis of radius of gyration k by proper subscript.)

μ Coefficient of viscosity

ν Kinematic viscosity

ρ Density (mass per unit volume)

Standard density of dry air, 0.12497 kg-m^{-4}-s^2 at 15° C and 760 mm; or 0.002378 lb-ft^{-4} sec^2

Specific weight of "standard" air, 1.2255 kg/m^3 or 0.07651 lb/cu ft

3. AERODYNAMIC SYMBOLS

S Area

S_w Area of wing

G Gap

b Span

c Chord

A Aspect ratio, $\frac{b^2}{S}$

V True air speed

q Dynamic pressure, $\frac{1}{2}\rho V^2$

L Lift, absolute coefficient $C_L=\frac{L}{qS}$

D Drag, absolute coefficient $C_D=\frac{D}{qS}$

D_0 Profile drag, absolute coefficient $C_{D_0}=\frac{D_0}{qS}$

D_i Induced drag, absolute coefficient $C_{D_i}=\frac{D_i}{qS}$

D_p Parasite drag, absolute coefficient $C_{D_p}=\frac{D_p}{qS}$

C Cross-wind force, absolute coefficient $C_C=\frac{C}{qS}$

i_w Angle of setting of wings (relative to thrust line)

i_t Angle of stabilizer setting (relative to thrust line)

Q Resultant moment

Ω Resultant angular velocity

R Reynolds number, $\rho\frac{Vl}{\mu}$ where l is a linear dimension (e.g., for an airfoil of 1.0 ft chord, 100 mph, standard pressure at 15° C, the corresponding Reynolds number is 935,400; or for an airfoil of 1.0 m chord, 100 mps, the corresponding Reynolds number is 6,865,000)

α Angle of attack

ϵ Angle of downwash

α_0 Angle of attack, infinite aspect ratio

α_i Angle of attack, induced

α_a Angle of attack, absolute (measured from zero-lift position)

γ Flight-path angle

REPORT No. 748

NORMAL-PRESSURE TESTS OF RECTANGULAR PLATES

By WALTER RAMBERG, ALBERT E. McPHERSON, and SAMUEL LEVY

National Bureau of Standards

NATIONAL ADVISORY COMMITTEE FOR AERONAUTICS

HEADQUARTERS, 1500 NEW HAMPSHIRE AVENUE NW., WASHINGTON, D. C.

Created by act of Congress approved March 3, 1915, for the supervision and direction of the scientific body of the problems of flight (U. S. Code, title 50, sec. 151). Its membership was increased to 15 by act approved March 2, 1929. The members are appointed by the President, and serve as such without compensation.

JEROME C. HUNSAKER, Sc. D., *Chairman*,
Cambridge, Mass.

GEORGE J. MEAD, Sc. D., *Vice Chairman*,
Washington, D. C.

CHARLES G. ABBOT, Sc. D.,
Secretary, Smithsonian Institution.

HENRY H. ARNOLD, Lieut. General, United States Army,
Commanding General, Army Air Forces, War Department.

LYMAN J. BRIGGS, Ph. D.,
Director, National Bureau of Standards.

W. A. M. BURDEN,
Special Assistant to the Secretary of Commerce.

VANNEVAR BUSH, Sc. D., Director,
Office Scientific Research and Development,
Washington, D. C.

WILLIAM F. DURAND, Ph. D.,
Stanford University, Calif.

O. P. ECHOLS, Major General, United States Army, Commanding General, The Matériel Command, Army Air Forces, War Department.

SYDNEY M. KRAUS, Captain, United States Navy, Bureau of Aeronautics, Navy Department.

FRANCES W. REICHELDERFER, Sc. D.,
Chief, United States Weather Bureau.

JOHN H. TOWERS, Rear Admiral, United States Navy,
Chief, Bureau of Aeronautics, Navy Department.

EDWARD WARNER, Sc. D.,
Civil Aeronautics Board,
Washington, D. C.

ORVILLE WRIGHT, Sc. D.,
Dayton, Ohio.

THEODORE P. WRIGHT, Sc. D.,
Asst. Chief, Aircraft Branch,
War Production Board.

GEORGE W. LEWIS, *Director of Aeronautical Research* — JOHN F. VICTORY, *Secretary*

HENRY J. E. REID, *Engineer-in-Charge, Langley Memorial Aeronautical Laboratory, Langley Field, Va.*

SMITH J. DEFRANCE, *Engineer-in-Charge, Ames Aeronautical Laboratory, Moffet Field, Calif.*

EDWARD R. SHARP, *Administrative Officer, Aircraft Engine Research Laboratory, Cleveland Airport, Cleveland, Ohio*

TECHNICAL COMMITTEES

AERODYNAMICS
POWER PLANTS FOR AIRCRAFT
AIRCRAFT MATERIALS
AIRCRAFT STRUCTURES
INVENTIONS & DESIGNS
OPERATING PROBLEMS

Coordination of Research Needs of Military and Civil Aviation

Preparation of Research Programs

Allocation of Problems

Prevention of Duplication

Consideration of Inventions

LANGLEY MEMORIAL AERONAUTICAL LABORATORY

LANGLEY FIELD, VA.

AMES AERONAUTICAL LABORATORY

MOFFETT FIELD, CALIF.

AIRCRAFT ENGINE RESEARCH LABORATORY

CLEVELAND AIRPORT, CLEVELAND, OHIO

Conduct, under unified control, for all agencies, of scientific research on the fundamental problems of flight.

OFFICE OF AERONAUTICAL INTELLIGENCE

WASHINGTON, D. C.

Collection, classification, compilation, and dissemination of scientific and technical information on aeronautics

REPORT No. 748

NORMAL-PRESSURE TESTS OF RECTANGULAR PLATES

By Walter Ramberg, Albert E. McPherson, and Samuel Levy

SUMMARY

Normal-pressure tests were made of 56 rectangular plates with clamped edges and of 5 plates with freely supported edges. Pressure was applied and the center deflection and the permanent set at the center were measured. For some of the plates, strains and contours were measured in addition.

The observed relation between center deflection and pressure for the plates with clamped edges was qualitatively in agreement with theory in so far as the deflection increased linearly with the pressure at very low loads and then increased more slowly as the membrane stresses became important. Quantitative agreement within ±10 percent for the linear portion of the deflection-pressure curve was obtained for only about one-fourth of the plates. The deviations for the rest of the plates were ascribed to deviations from the theoretical clamping conditions at the edges.

With the beginning of permanent set both the total deflection and the permanent set at the center of the plates with clamped edges increased linearly with the pressure for most of the plates. Extreme-fiber strains measured at the center of three square plates were in approximate agreement with calculated values.

Washboarding pressures were determined for three cases: the pressure for a set at the center of 1/500 the span of the plate, the pressure for a set at the center of 1/200 the span of the plate, and the Navy yield pressure. The Navy yield pressure was obtained from a plot of permanent set against pressure by determining the intersection with the pressure axis of a straight line faired through the plotted points.

The measured Navy yield pressure and the pressures for a set of 1/500 the span for the plates with clamped edges were between the theoretical pressure, for yielding at the edge and for yielding at the center, for more than 80 percent of the plates. There was a tendency to shift from the first curve to the second with increasing ratio of span to thickness, indicating that the thick plates tended to yield by bending near the edges while the very thin plates yielded more like a membrane throughout the plate. The pressures for a set of 1/200 the span were in agreement with the theoretical pressure for yielding at the center of the plate.

The measured center deflections of five plates with freely supported edges at low loads were between 0 and 20 percent less than those calculated from Kaiser's theory. The theory does not extend to sufficiently high center deflections to make possible a calculation of washboarding pressures on the same basis as for the plates with clamped edges. Furthermore, the tests were too few to provide empirical relations of any generality. The washboarding pressures for the plates tested were approximately the same as the washboarding pressures for the clamped-edge plates.

INTRODUCTION

An investigation of the strength of flat plates under normal pressure has been conducted for several years at the National Bureau of Standards with the support of the Bureau of Aeronautics, Navy Department. Information on this subject was desired by the Bureau of Aeronautics because of its bearing on the design of seaplanes. Seaplanes are subject to a severe impact during landing and take-off, especially on rough water. The impact must be withstood first by the bottom plating and then by a system of transverse and longitudinal members to which the bottom plating is attached, before it is carried into the body of the structure. Published experimental estimates for the maximum pressure experienced during landing and take-off range from 4.65 pounds per square inch (reference 1) to 6.3 pounds per square inch (reference 2), while Wagner (reference 3) found theoretically that impact pressures as high as 4 atmospheres or about 60 pounds per square inch may be possible for certain shapes of float bottom.

The bottom should be strong enough not to dish in or "washboard" permanently under these impact pressures. Such washboarding is undesirable both because of the increased friction between the float bottom and the water and because of the increased aerodynamical drag in flight.

The bottom plating of seaplanes is, as a rule, subdivided into a large number of nearly rectangular areas by the transverse and longitudinal supporting ribs. Each of these areas will behave substantially like a rectangular plate under normal pressure. Normal-pressure tests of rectangular plates may therefore be

Aero 12 Dec. '45

used to study the washboarding of seaplane bottoms provided that the plates are loaded and are held at the edges just as in the seaplane.

Impact pressure is assumed to be nearly uniform over a portion of sheet covering several rectangular fields. Under these conditions the sheet is subjected to a hydrostatic normal pressure equal to the average impact pressure in the region considered. The behavior of the sheet approximates that in an infinite sheet supported on a homogeneous elastic network with rectangular fields of the same rigidity as the supporting framework of the seaplane.

The displacement in the plane of the sheet and the slope of the sheet relative to the plane of the network must be zero from symmetry wherever the sheet passes over the center line of each supporting beam. Each rectangular field will therefore behave as a rectangular plate clamped along its four edges on supports that are rigid enough in the plane of the sheet to prevent their displacement in that plane. At the same time these supports must have a rigidity normal to the plane of the sheet equal to that of the actual supports in the seaplane bottom. The rigidity of the supports will lie somewhere between the unattainable extremes of zero rigidity and infinite rigidity. The extreme of infinite rigidity normal to the plane of the sheet is one that may be approximated in actual designs and, furthermore, it is a case that can be experimentally investigated by clamping rectangular plates in a rigid framework and subjecting them to normal pressure. It is probable that the stress distribution in such a fixed-edge plate will, in most cases, be less favorable than the stress distribution in the elastic-edge plate. The strength of plates obtained from the tests will therefore be on the safe side if applied in seaplane design. Reference might be made in this connection to a paper by Mesnager (reference 4) in which it is shown that a rectangular plate with elastic edges of a certain flexibility will be less highly stressed than a clamped-edge plate.

Considerations of this nature led to the decision to test rectangular plates of various materials, thicknesses, and ratios of length to width by holding their edges clamped in a rigid frame and subjecting them to hydrostatic pressure. It was decided also to subject to normal pressure some plates with freely supported edges. It was felt that this type of deformation would approximate the deformation in a rectangular panel of the bottom plating resisting a higher impact pressure than the surrounding panels and supported on beams of torsional stiffness insufficient to develop large moments along the edges. The high bending stresses at the edges characteristic of rigidly clamped plates would then be absent.

SPECIMENS

Dimensions and tensile properties for the plates tested with clamped edges are given in table 1 and for plates with freely supported edges in table 2. Tests with clamped edges were made on 39 plates of 17S–T aluminum alloy ranging in thickness from 0.0104 to 0.1000 inch and in size from 2.5 by 2.5 to 7.5 by 17.5 inches; on 12 plates of 18:8 stainless steel ranging in thickness from 0.0127 to 0.0601 inch and in size from 2.5 by 2.5 to 5 by 5 inches; on 3 plates of 17S–RT aluminum alloy ranging in thickness from 0.0208 to 0.0384 inch and 2.5 by 7.5 inches in size; and on 2 plates of 24S–RT aluminum alloy 0.0204 and 0.0250 inch in thickness and 2.5 by 7.5 inches in size. The tests of plates with freely supported edges were confined to five 5- by 5-inch 17S–T aluminum-alloy plates 0.0292 to 0.0641 inch in thickness.

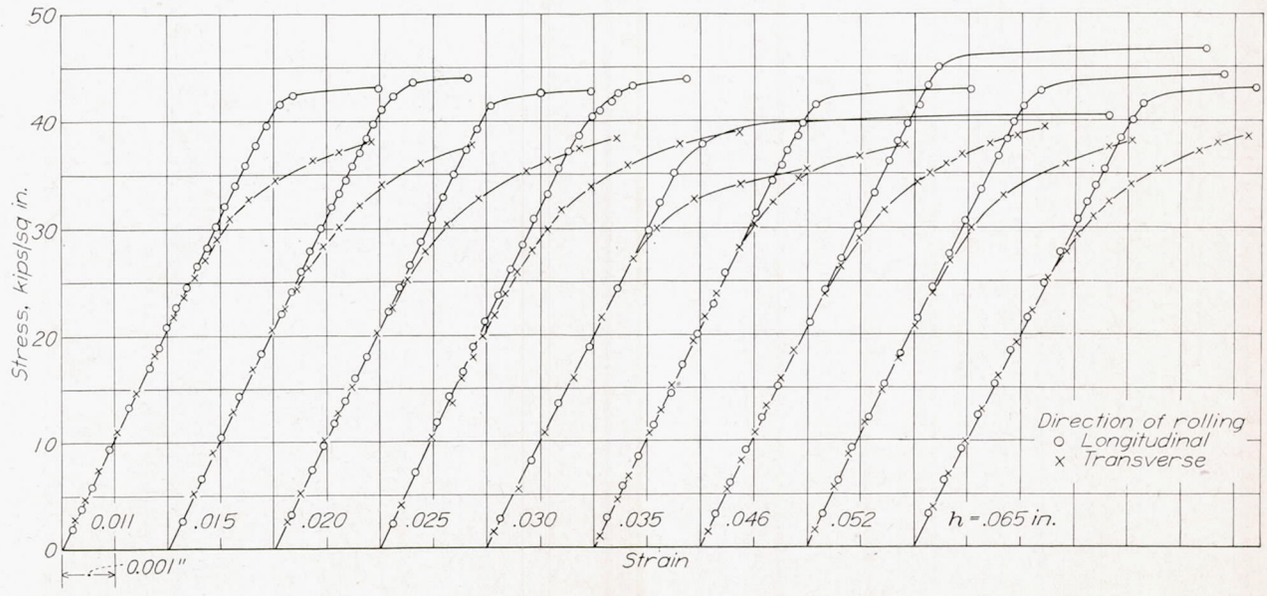

FIGURE 1.—Tensile stress-strain curves for 17S–T aluminum alloy.

Tensile properties were determined on coupons taken both longitudinally and transversely out of the sheet from which the plates had been cut. Typical stress-strain curves are shown for the 17S–T aluminum-alloy sheet in figure 1; for the 18:8 stainless steel in figure 2; and for the 17S–RT and 24S–RT aluminum alloy in figure 3. The yield strengths in the longitudinal and transverse directions are given in tables 1 and 2.

The difference in plastic behavior of the aluminum alloy and the stainless steel is immediately apparent from the stress-strain curves. A stress-strain curve for a longitudinal coupon of the aluminum alloy has a relatively sharp knee near the yield point; the tensile properties are nearly independent of thickness; the tensile properties are consistently higher in the longitudinal direction than in the transverse direction. The stress-strain curves of the stainless steel are curved beginning at very low stresses and there is no pronounced knee near the yield point; the tensile properties increase rapidly as the thickness of the material decreases; the material is roughly isotropic in tension, the yield strengths being nearly the same in both longitudinal and transverse directions.

It was felt that the inclusion of such widely divergent materials would indicate the effect of the shape of the stress-strain curve on the behavior of the plates.

TESTS

LOADING

The apparatus for subjecting rectangular plates to normal pressure is shown in figure 4. The plate A was mounted on top of a 3- by 50- by 100-inch steel base

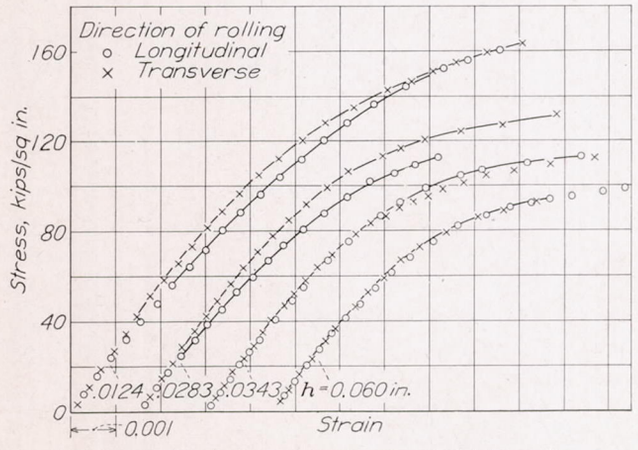

FIGURE 2.—Tensile stress-strain curves for 18:8 stainless steel.

plate with provision for testing plates that range in size from 2.5 by 2.5 inches to 30 by 90 inches. Pressure was applied by the hand pump B and was transmitted to the bottom side of the plate through the copper tube C attached to a hole in the steel base plate. Water was used as a pressure-transmitting fluid. The pressure under the plate was measured by connecting one of the pressure gages D, E, or F to the copper tube H attached to a second hole in the steel base plate. (See also fig. 6.) Pressure gage D was a U-tube for measuring pressures from 1 to 20 pounds per square inch; F was a Bourdon tube gage for measuring pressures from 20 to 100 pounds per square inch; and E was a Bourdon tube gage for measuring pressures from 100 to 300 pounds per square inch. The error in reading pressures was estimated as less than 0.1 pound

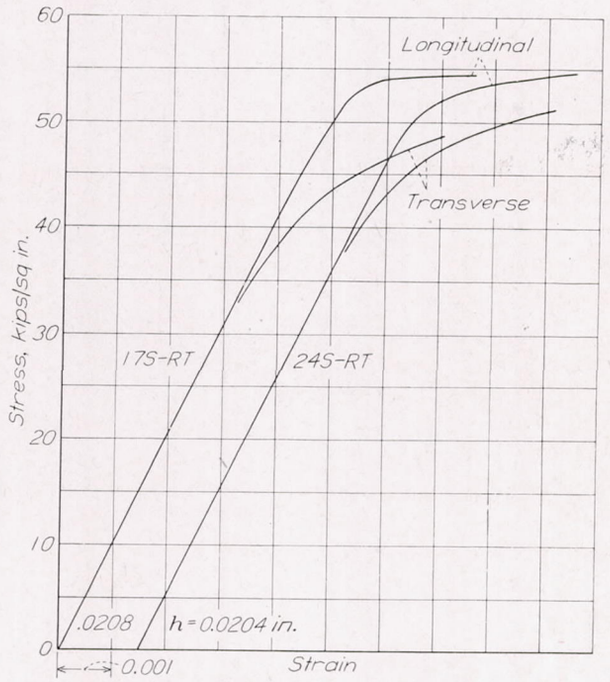

FIGURE 3.—Tensile stress-strain curves for 17S–RT and 24S–RT aluminum alloy.

per square inch in the case of the U-tube and less than 1 pound per square inch in the case of the Bourdon tube gages. Approximate values of pressure above 300 pounds per square inch were obtained from a Bourdon tube gage that could be mounted at G on the hand pump.

The method of mounting the plate with clamped edges is shown in figures 5 and 6. The rubber membrane J was supported near the lower surface of the specimen by means of the wood frame M (fig. 6). A watertight joint between the membrane and the base plate I was obtained by applying rubber cement to the base plate and holding the membrane down by means of the lower clamp bar K, which was fastened to the base plate with flathead screws. The plate A was cut to allow a grip of ¾ inch between the clamp bars K and L. The upper bar L was leveled relative to K by means of spacers N cut from the same material as the plate. The gripping faces of the bars K and L were knurled to reduce slipping. The assembly of clamp bars, plate, and membrane were held to the base plate I by means of ¾-inch United States Standard capscrews drawn up with a torque of about 500 pound-inches.

In the case of the plates tested with freely supported

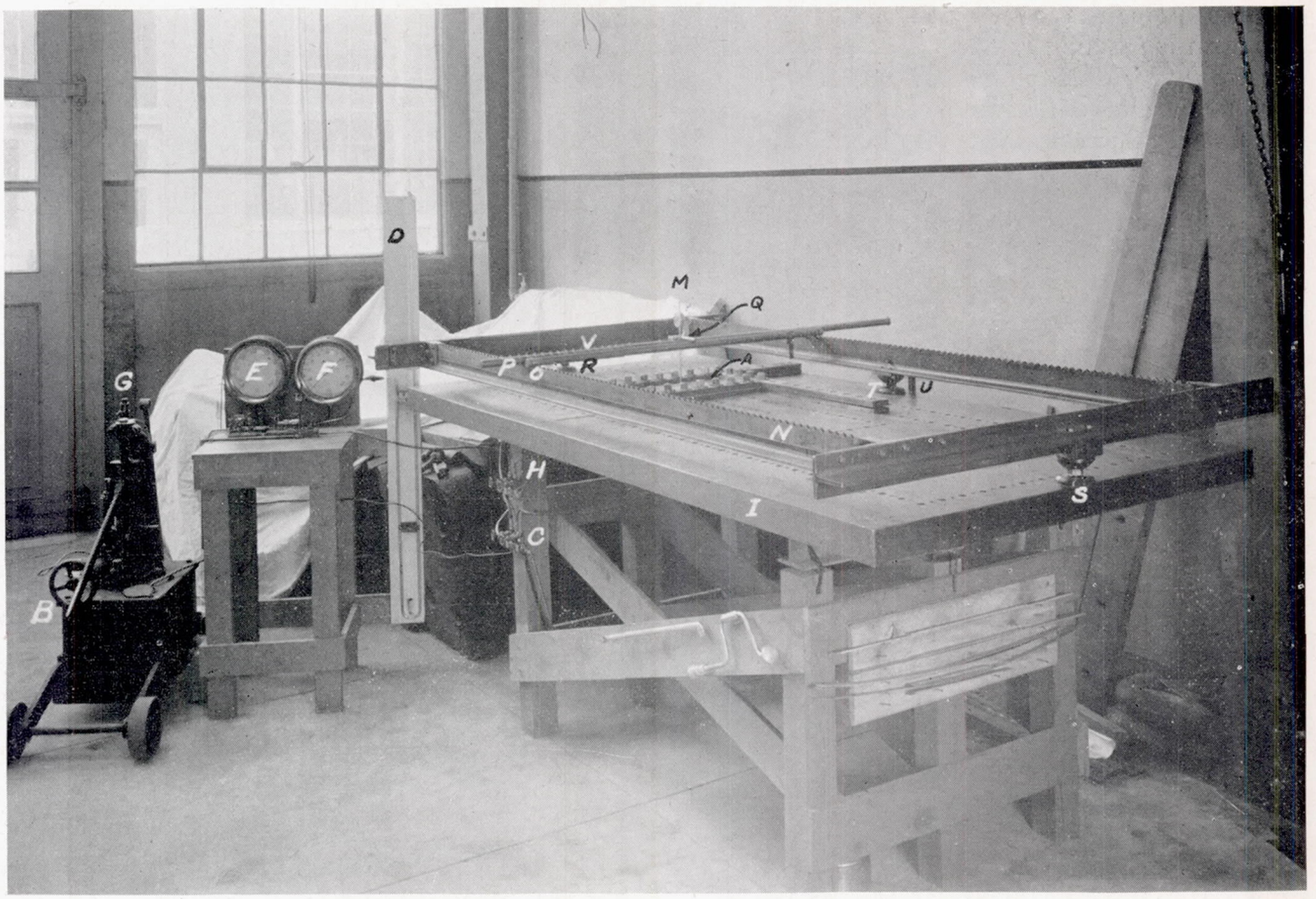

FIGURE 4.—Apparatus for normal-pressure tests of rectangular plates.

edges, the same clamping procedure was applied except that the bars K (fig. 6) were turned through 180° in a horizontal plane so that the plate would be able to tilt into the groove shown in the outer portion of K in figure 6. The spacer N in this case extended on both sides of the bolts. This arrangement, it was believed, would approximate the theoretical edge condition of zero displacement and zero bending moment that was assumed to hold for a plate with freely supported edges.

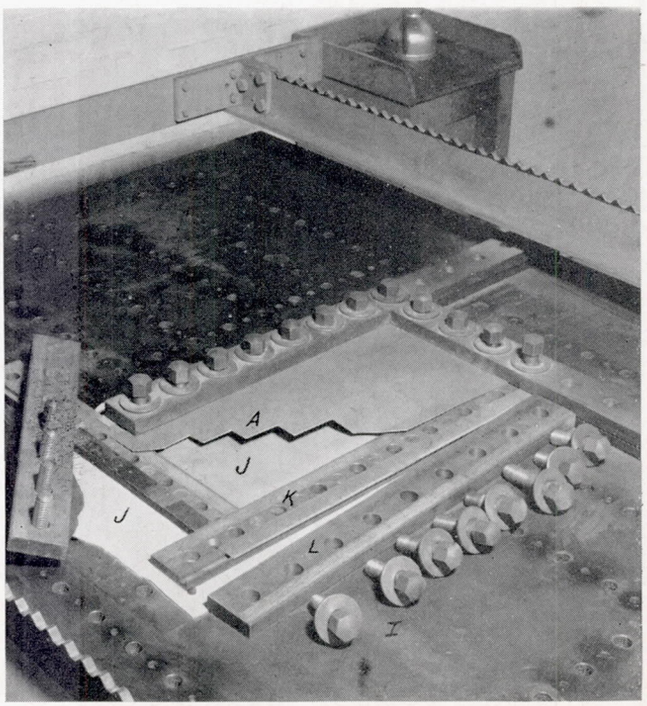

FIGURE 5.—Cut-away plate showing method of clamping plate in testing apparatus

The test data for a given plate obtained with this apparatus showed consistent behavior in that the scatter of observed points about a curve faired through them was small. There were large and erratic deviations from the expected behavior for curves obtained for nominally identical or, at least, similar plates. These deviations were ascribed to uncertainties in the condition of clamping and, in fact, led to the tests of circular plates with clamped edges already reported (reference 5) in which additional precautions were taken to approach a condition of rigid clamping. The precautions were justified, leading to a more consistent set of test data. (See reference 5, figs. 28 to 36.)

The following specific deviations from ideal test procedure may be responsible for the erratic results obtained with the rectangular plates with clamped edges:

A. The setting up of initial tension or compression in the plate during the clamping in the fixture

B. Rotation of the clamping bars K and L on the elastic foundation provided by the rubber membrane J

C. Deviation from flatness at no load

D. Slipping of the plate between the clamping bars K and L

E. The setting up of local clamping stresses at the edges due to deviation from uniform clamping.

In the case of the plates with supported edges there is, in addition, the possibility of

F. Edge bending moments applied by the clamping bars.

A measure of the smallness of the deviation B was obtained by clamping a 2.5- by 7.5-inch aluminum-alloy plate in the fixture and measuring the angular rotation of the clamping bars K as the pressure was increased from 5 to 250 pounds per square inch. The rotation was found to be of the order of 1.2×10^{-6} radian per pound per square inch. Since the measured angular rotation at the middle of the long edges of a 0.1- by 2.5- by 7.5-inch plate of aluminum alloy with freely supported edges when bent by normal pressure was about 200 times this value and since the plates included in the test program were generally less rigid than a 0.1-inch aluminum-alloy plate, it was concluded that the deviation B from ideal clamping could be neglected.

The deviations A, C, D, E, and F are too indefinite for analytical treatment analogous to the treatment of the deviations for the circular plates (appendixes A to D of reference 5). The best check that could be made was to estimate their combined effect by comparing the observed center deflection w_o with theoretical values w_{oo} for corresponding pressures. The procedure used is described in detail in a later part of this paper. It led to the relative deviations

$$\frac{w_o-w_{oo}}{w_{oo}}=\frac{\Delta w_o}{w_{oo}}$$

given in tables 3 and 4. The relative deviation was

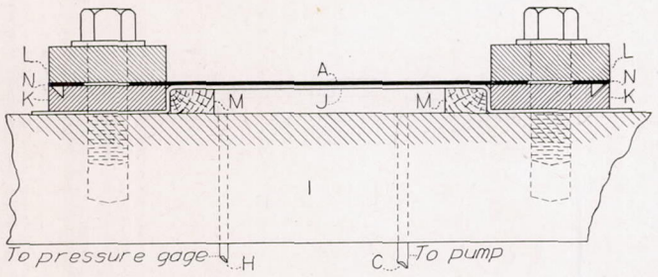

FIGURE 6.—Section through plate mounted for normal-pressure test with clamped edges.

between −0.10 and 0.10 for 27 percent of the plates with clamped edges. It was less than −0.10 or greater than 0.45 for 44 percent of the plates with clamped edges. In the case of the five plates with freely supported edges the relative deviations ranged from 0.00 to −0.20. The fact that the deviation was negative for all the plates indicates that the edge supports did partly resist rotation.

DEFLECTION

The deflections of the plates under load were measured with a $\frac{1}{1000}$-inch dial gage (M, fig. 4). The head of the dial gage was supported on the reference frame N by the two parallel bars O and P which rested, in turn, in triangular notches that had been

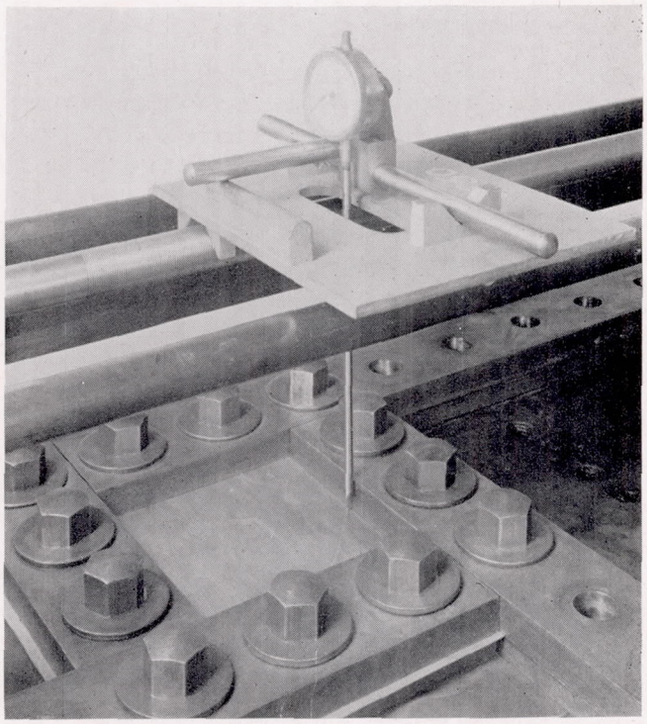

FIGURE 7.—Auxiliary platform for measuring deflections at points 1/20 inch apart.

cut in the reference frame at 1-inch intervals. The reference frame N was connected to the base plate I by a point-line-plane support in order to avoid distortion of the frame by deformation of the base plate. The point support R consisted of a $\frac{5}{8}$-inch steel ball riding in conical seats on N and I; the line support S consisted of a second $\frac{5}{8}$-inch ball riding in a groove on I, the axis of which passed through R; and the plane support T consisted of a third $\frac{5}{8}$-inch ball riding on a plane on I. A counterweight at U prevented the reference frame from tipping about a line through R and S.

The plunger of the dial gage M was alined normal to the base plate I by rotating the dial gage bar P until the horizontal arm Q attached to M rested on the parallel bar O. The position of the plunger point could be moved at 1-inch intervals in a longitudinal direction by moving the two bars O and P to different notches in the reference frame N. They could be moved in set intervals (usually 1-in. intervals) in a transverse direction by bringing a different one of the positioning rings V on P in contact with the flat outside surface of notched bars N.

For closer interval spacing of the dial readings the platform shown in figure 7 was placed on the bars O and P. With this platform, longitudinal and trans-

verse displacements at 1/20-inch intervals were made possible by the use of knife edges resting in V-shaped grooves accurately spaced in 1/20-inch intervals.

The reference frame N with its point-line-plane support operated very satisfactorily throughout the series of tests. Dial readings were always found to return to the same value within 0.001 inch even after violent disturbance of the test set-up.

Figure 8 shows the change in shape of the deflection curve along the center line of square plate 34 with clamped edges as the pressure is increased to a value producing a deflection at the center equal to about 1.8 times the thickness of the plate. Curves are included from the data of references 6 and 7. With increasing pressure the reversed curvature due to the

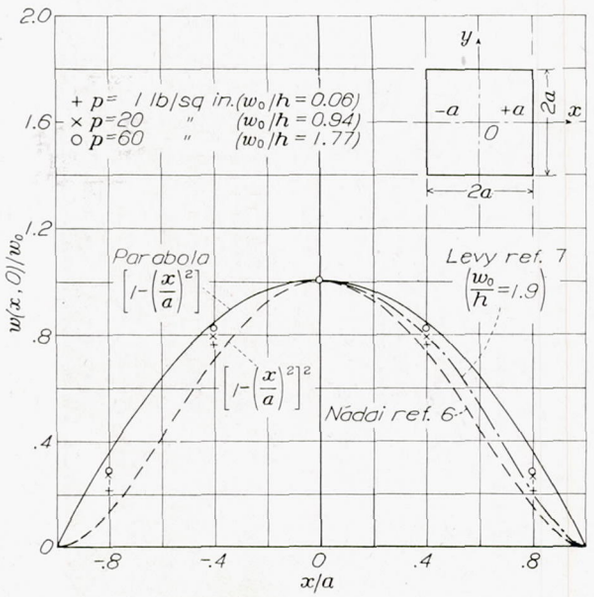

FIGURE 8.—Change in shape of deflection curve along center line as the pressure is increased for clamped edge square plate 34. h, 0.0653 inch; a, 2.5 inches.

clamping moments was reduced and the deflection curve approached a parabola.

The corresponding curves for square plate 60 with freely supported edges are shown in figure 9, with curves from references 8 and 9. In this case the deflection curve approached a parabola for low loads, just as for a simple beam under a uniformly distributed load. At the high pressures the curvature in the center of the plate became less than that corresponding to such a parabola.

The deflection curve along the longitudinal center line of a 0.0529- by 7.5-by 17.5- inch 17S–T plate is shown in figure 10. It is seen that the end effect due to clamping along the short edges of the plate extended a distance into the plate equal to about one plate span. It may be concluded that the center deflection of a rectangular plate having a length equal to twice its width approximates that for an infinite-plate strip.

The center deflection and the permanent set at the center were measured for each one of the plates tested as the pressure was increased from a low value to one at which the permanent set at the center attained the same order of magnitude as the elastic deflection (center deflection minus permanent set). Figures 11 to 14 give the results for plates with clamped edges

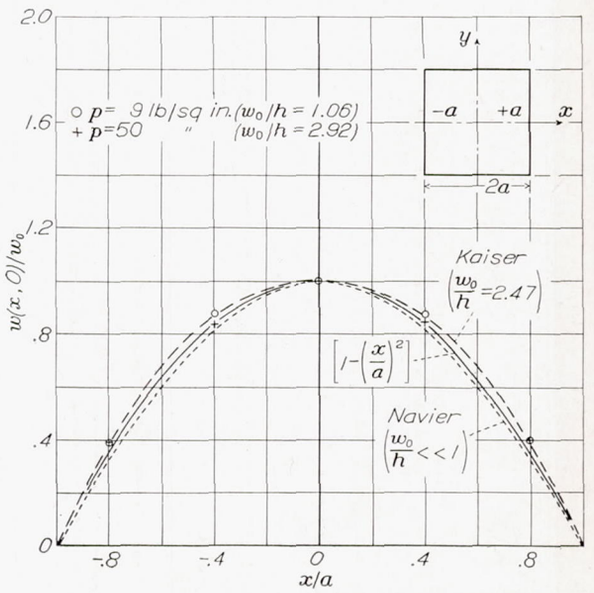

FIGURE 9.—Change in shape of deflection curve along center line as the pressure is increased for freely supported square plate 60. h, 0.641 inch; a, 2.5 inches.

and figure 15 gives the results for plates with freely supported edges.

At very low loads the center deflection was found to increase directly with the pressure, as for an ordinary

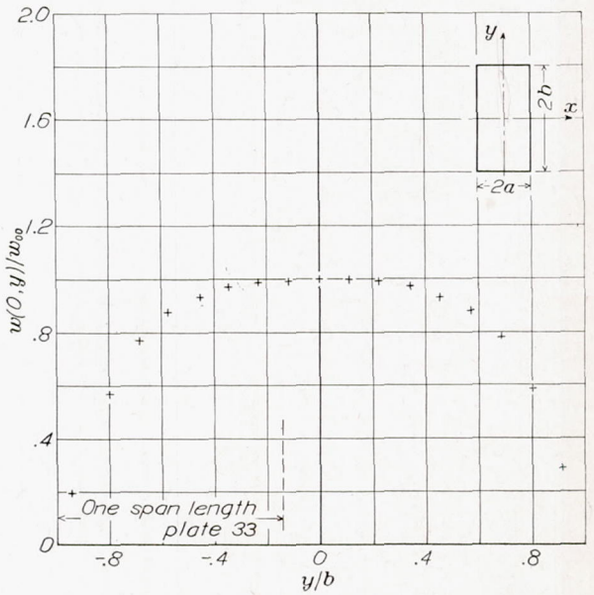

FIGURE 10.—Deflection curve along longitudinal center line of rectangular plate 33 (17S–T) with clamped edges. h, 0.0529 inch; $2a$, 7.5 inches; $2b$, 17.5 inches; w_0/h, 6.8; p, 50 pounds per square inch.

beam; it increased more slowly as the membrane stresses became important; and it approached a linear variation with pressure as yielding became pronounced. The permanent set at the center increased at an

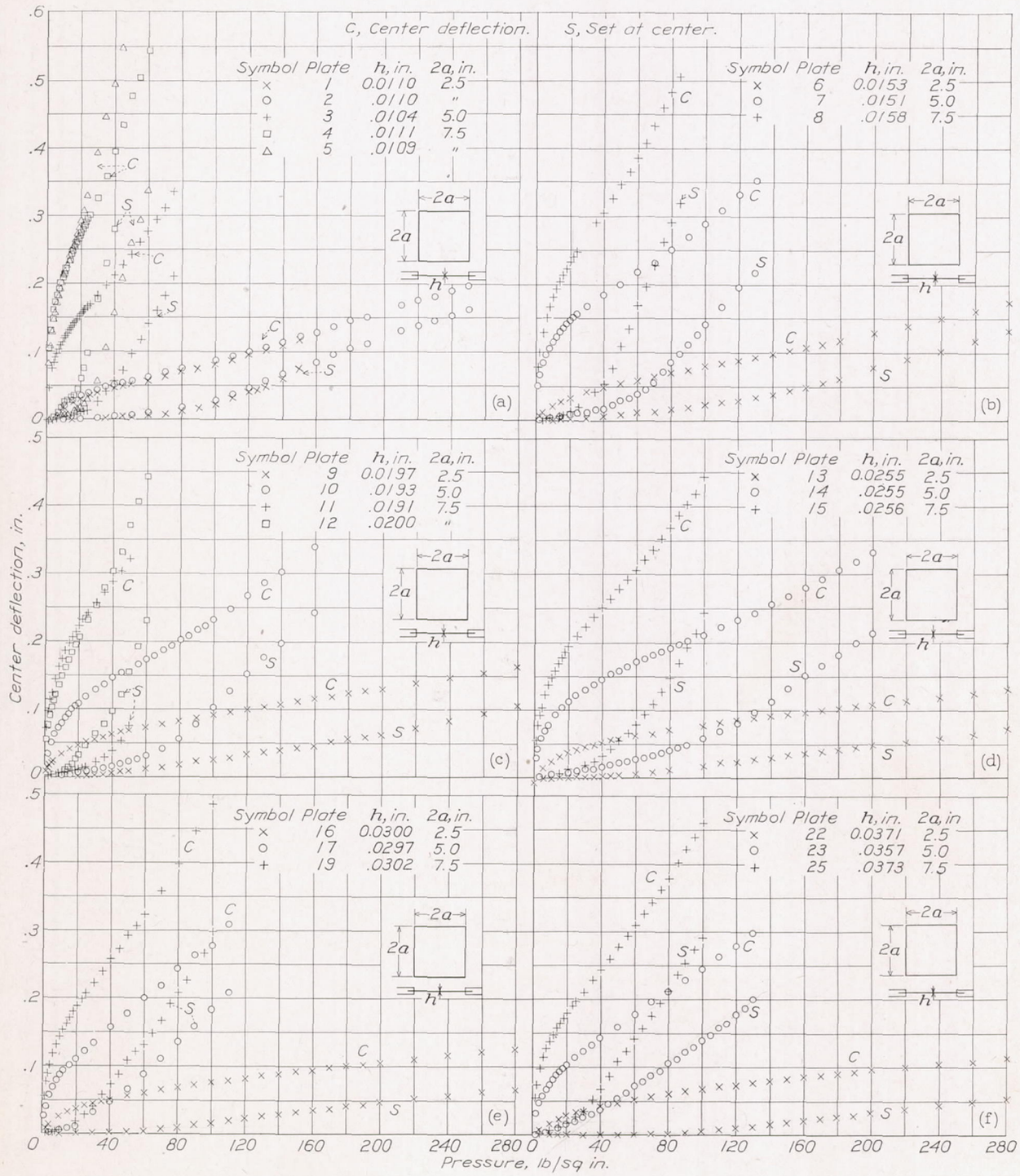

(a) Plates 1, 2, 3, 4, and 5.
(b) Plates 6, 7, and 8.
(c) Plates 9, 10, 11, and 12.
(d) Plates 13, 14, and 15.
(e) Plates 16, 17, and 19.
(f) Plates 22, 23, and 25.

FIGURE 11.—Deflection and set at center of 178–T aluminum-alloy plates with clamped edges.

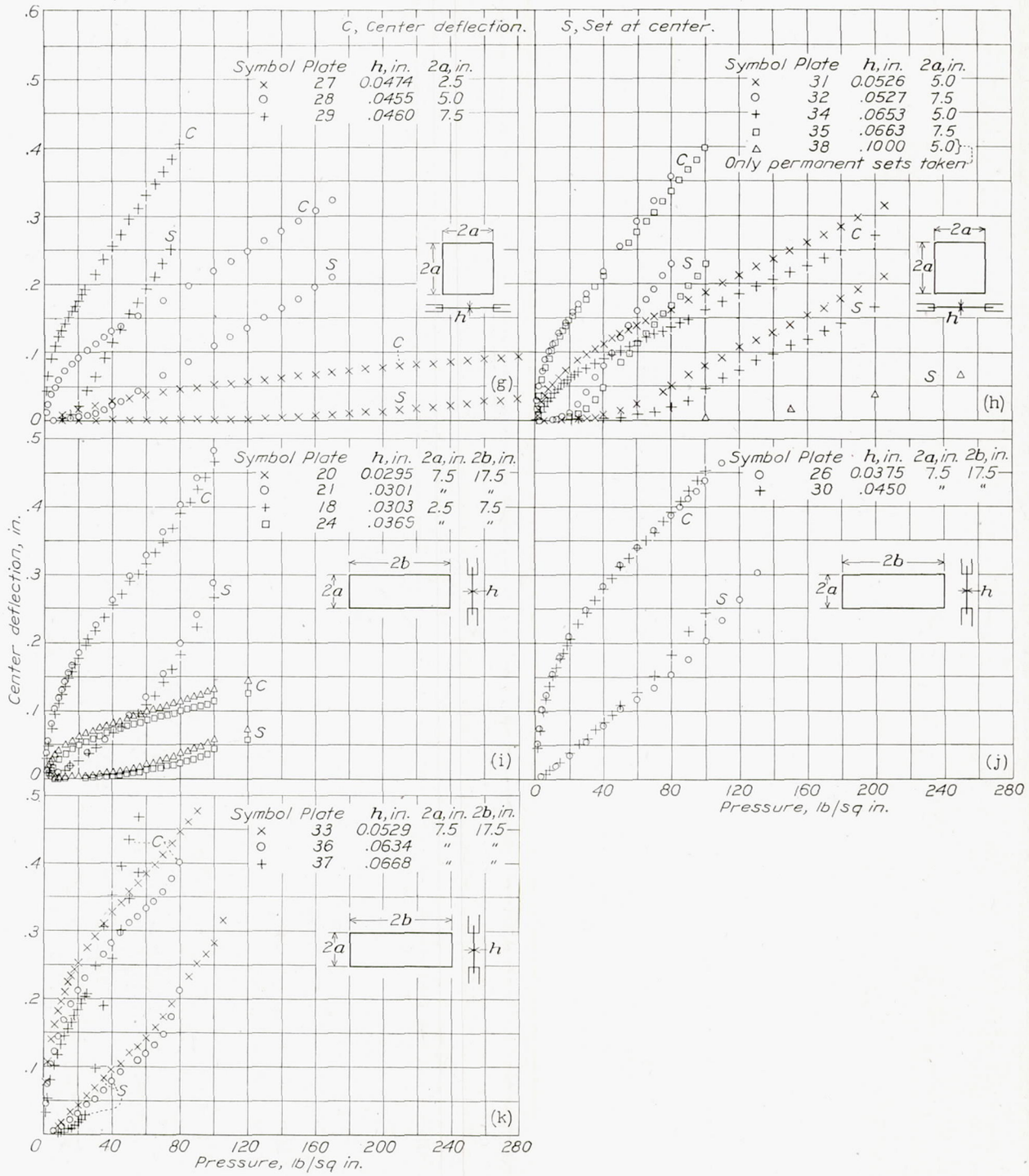

(g) Plates 27, 28, and 29.
(h) Plates 31, 32, 34, 35, and 38.
(i) Plates 18, 20, 21, and 24.
(j) Plates 26 and 30.
(k) Plates 33, 36, and 37.

FIGURE 11 Concluded.—Deflection and set at center of 17S–T aluminum-alloy plates with clamped edges.

increasing rate with increase in pressure and, in most plates, it approached a straight line having approximately the same slope as the asymptote to the deflection curve. In this respect the rectangular plates showed the same behavior as the circular plates plotted in figures 14 to 20 of reference 5.

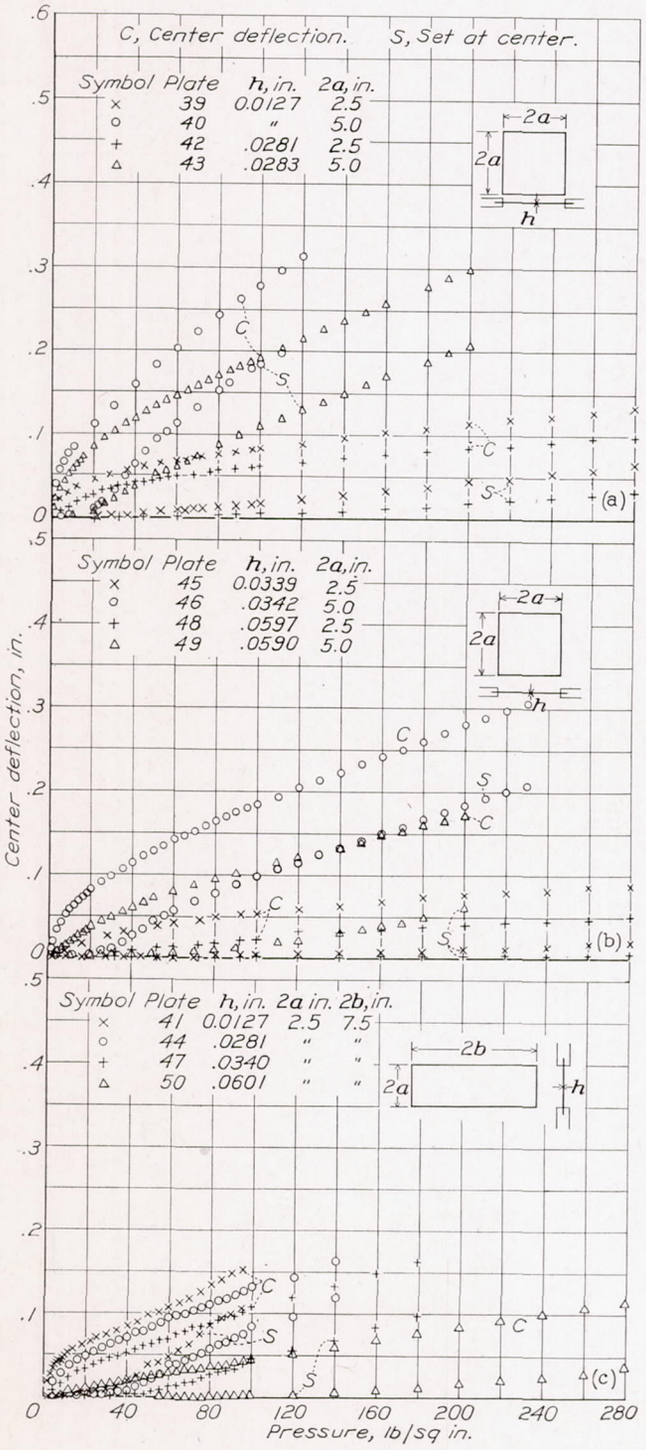

(a) Square plates 39, 40, 42, and 43.
(b) Square plates 45, 46, 48, and 49.
(c) Rectangular plates 41, 44, 47, and 50.

FIGURE 12.—Deflection and set at center of 18:8 stainless-steel plates with clamped edges.

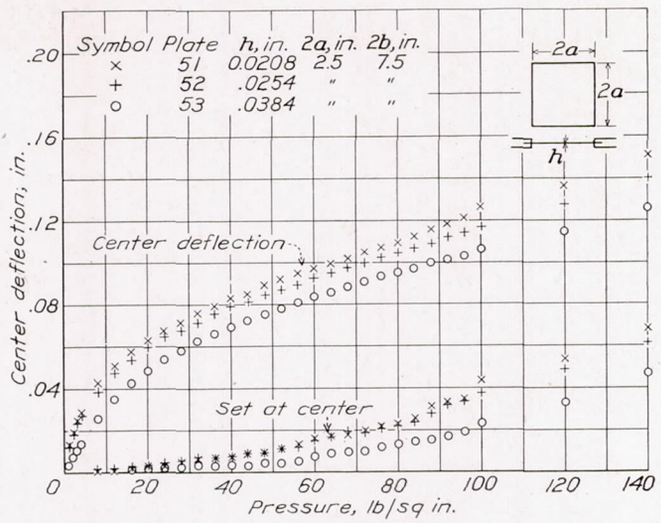

FIGURE 13.—Deflection and set at center of rectangular 17S–RT aluminum-alloy plates with clamped edges.

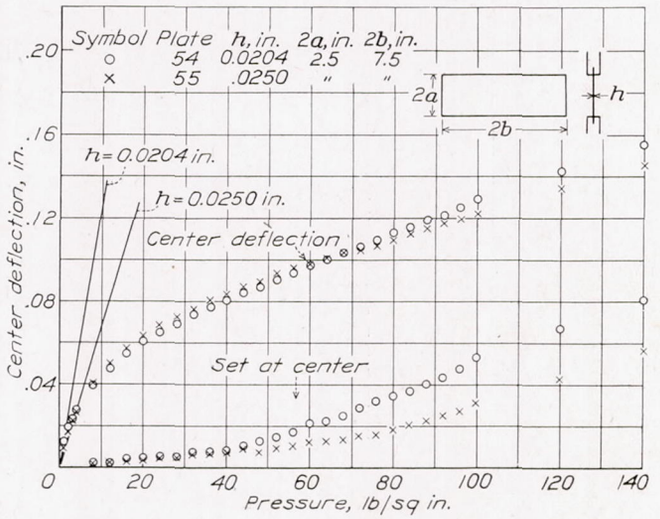

FIGURE 14.—Deflection and set at center of rectangular 24S–RT aluminum-alloy plates with clamped edges.

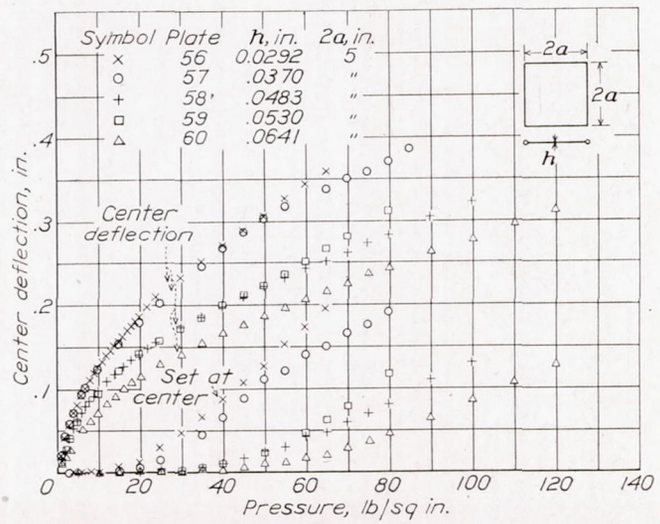

FIGURE 15.—Deflection and set at center of square 17S–T aluminum-alloy plates with freely supported edges.

In the case of plates 1 to 8 and plates 10, 12, 14, 15, 18, 20, 21, 25, 33, 36, and 37, the center-deflection curves deviated increasingly from their linear asymptote above a certain pressure so that there was an inflection point in the curves. The inflection point was ascribed to slipping of the plate between the clamps. In some of the plates this slipping could be confirmed by examining the clamped margin of the plate after the test. It is also borne out by the absence of such behavior in the circular plates (reference 5) in which particular pains were taken to obtain rigid clamping.

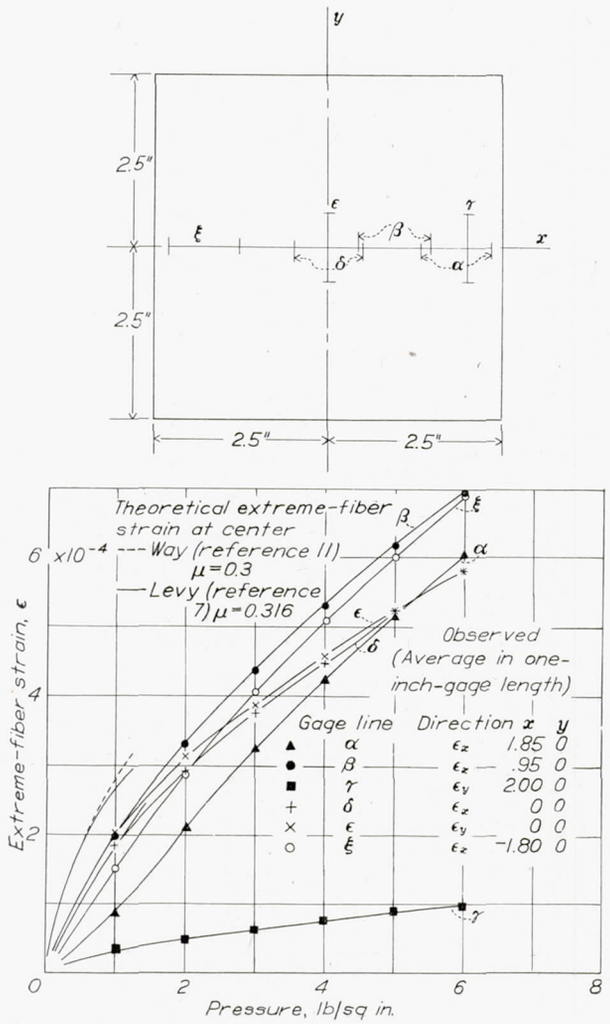

FIGURE 16.—Extreme-fiber strains on square 17S–T aluminum-alloy plate 10a with clamped edges.

The washboarding pressures, that is, the pressures producing permanent set in the plates, were measured just as in the case of the circular plates (reference 5) by the following three criterions:

1. The Navy yield pressure p_y, defined as the pressure corresponding to the intercept on the pressure axis of the asymptotic straight line for the set against pressure curve

2. The pressure $p_{2a/500}$ to produce a set at the center of 1/500 the span of the plate

3. The pressure $p_{2a/200}$ to produce a set at the center of 1/200 the span of the plate.

These three pressures are given in table 3 for the plates with clamped edges and in table 4 for the plates with freely supported edges. Minimum and maximum values are given for p_y in the case of the plates for which an accurate determination was not possible because the asymptote to the set against pressure curve was not clearly defined. The Navy yield pressure p_y exceeded $p_{2a/200}$ for only 5 plates; it was between $p_{2a/500}$ and $p_{2a/200}$ for half of the other plates and was less than $p_{2a/500}$ for the other half.

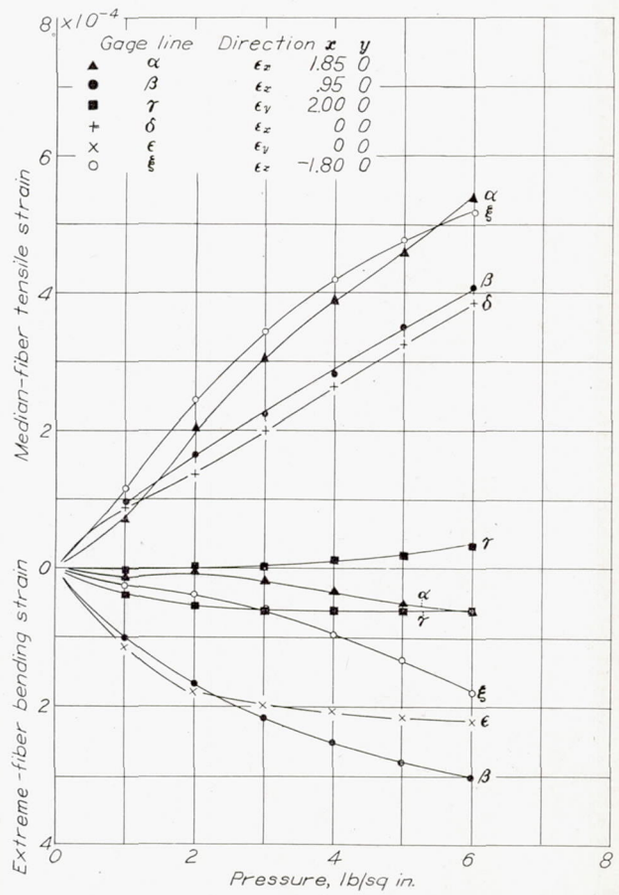

FIGURE 17.—Medium-fiber tensile strain and extreme-fiber bending strain (average over 1-in. gage length) for square 17S–T aluminum-alloy plate 10a with clamped edges.

STRAIN

Surface strains for plates 10a and 34 were measured with 1-inch Tuckerman strain gages placed directly on the surface of the plate. (See fig. 21 of reference 5.) The strain readings were corrected for the apparent strain due to bowing of the plate between gage points by adding a term $\frac{1}{24}\left(\frac{l}{r}\right)^2$ (see reference 10, p. 6) where $l=1$ inch is the gage length and r is the average radius of curvature of the plate between gage points (obtained from the measured contour of the plate).

The results for the 5- by 5- by 0.0202-inch aluminum-alloy plate 10a with clamped edges are given in figures

16, 17, and 18. Figure 16 shows surface strains at six gage lines for pressures from 1 to 6 pounds per square inch; these pressures were below the washboarding pressures of the plate (31 to 58 lb/sq in.). Unfortunately, the gage length of 1 inch was too great to show the reversal in extreme-fiber bending strain and its increase to a maximum value of opposite sign at the clamped edges. Measurements over small gage lengths or with a number of overlapping gage lines, such as those made on circular plates (reference 5) would be required for an adequate description of the spanwise strain distribu-

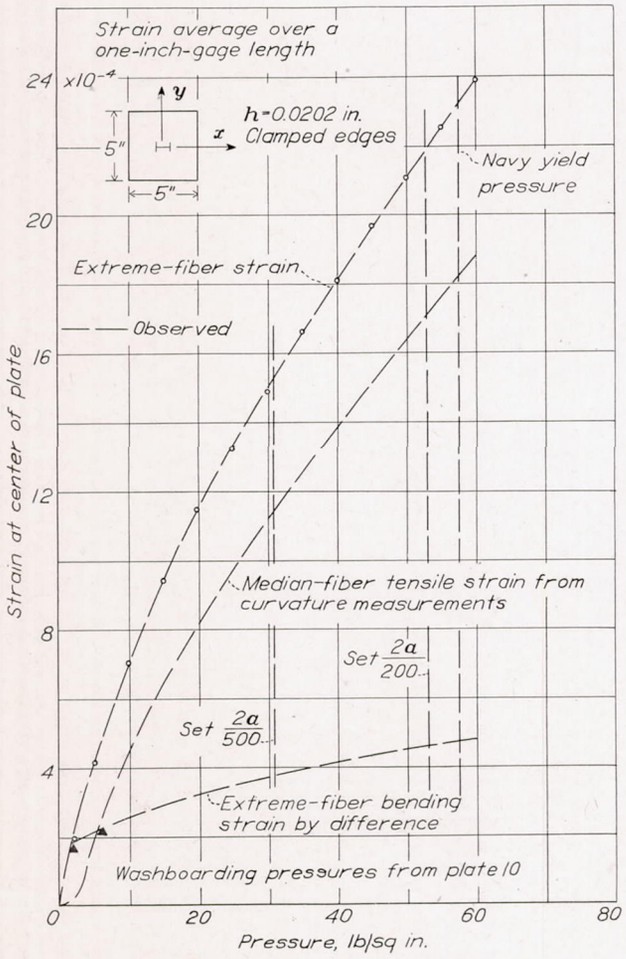

FIGURE 18.—Strain at center of square 17S–T aluminum-alloy plate 10a (average over 1-in. gage length).

tion. Curves from references 7 and 11 are included in figure 16. The strain-against-pressure curves are similar to the deflection-against-pressure curves in so far as the slope decreases with increasing pressure. The explanation, in both cases, is the same. At very low pressures the entire load was carried in bending but, as the deflection increased, catenary tension developed and an increasing proportion of the load was carried by catenary action.

This action is brought out quantitatively in figure 17 by the separation of the surface strain into median-fiber tensile strain and extreme-fiber bending strain. The extreme-fiber bending strain was calculated for this purpose from the measured contour of the plate as the ratio of distance of extreme fiber from the neutral plane of the plate to average radius of curvature along the gage line. The median-fiber strain was calculated as the surface strain minus the bending strain. The ratio of bending strain to median-fiber strain decreased with in-

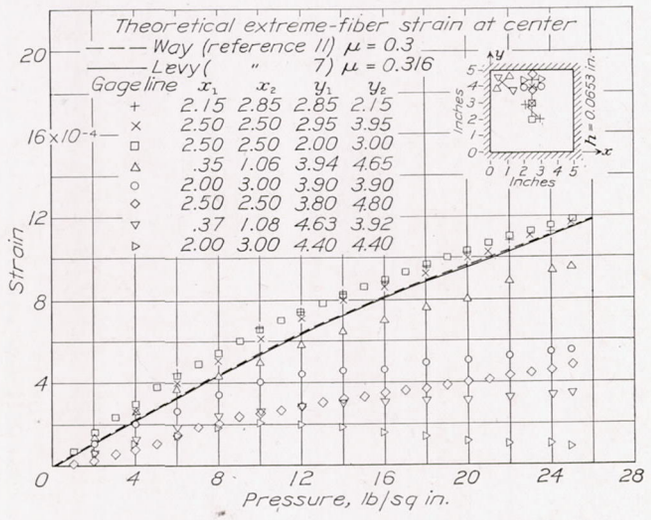

FIGURE 19.—Extreme-fiber strains (average over 1-in. gage length) of 17S–T aluminum alloy plate 34.

creasing pressure except for gage line ξ. The bending strain was smaller than the median-fiber strain at a pressure of 6 pounds per square inch for all gage lines except γ. At pressures in excess of 6 pounds per square inch the strain was read only at the center of the plate. The results are given in figure 18.

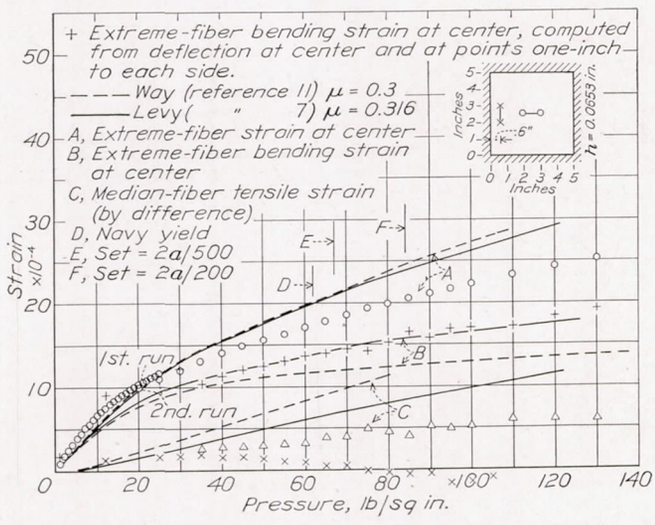

FIGURE 20.—Strain at center and edge of 17S–T aluminum-alloy plate 34 (average over 1-in. gage length).

Strains for the 5- by 5- by 0.0653-inch 17S–T aluminum-alloy plate 34 with clamped edges are given in figures 19 and 20. Figure 19 shows extreme-fiber strains for eight gage lines at pressures from 1 to 25 pounds per square inch; these pressures were below the washboarding pressures of 62 to 84 pounds per square

inch obtained for this plate. Measurements above 25 pounds per square inch were made only on a center gage line and an edge gage line. The results are given in figure 20 for pressures up to 130 pounds per square inch. The curve for strain at the center of the plate resembles that for plate 10a in so far as it shows a decrease in slope with increasing pressure.

Curvature measurements were made on three of the five 5- by 5-inch 17S–T aluminum-alloy plates with freely supported edges. Normal-pressure tests of the first two plates with freely supported edges had indicated that yielding might be due to the development of a diagonal fold at each one of the four corners, which, in turn, seemed to be caused by pulling out of the plate from the supports near the corners. Curvature was accordingly measured at both the center of the plate and across the diagonal near one or two of the corners. The extreme-fiber strains for these gage lines are plotted

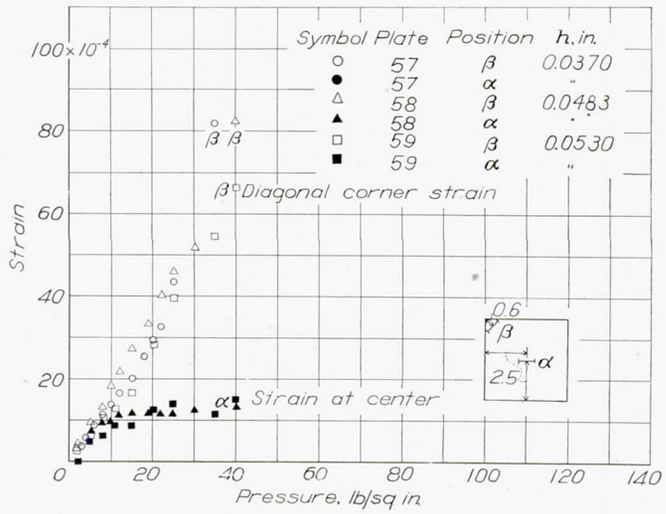

FIGURE 21.—Extreme-fiber bending strains from 1-inch spherometer for 5- by 5-inch 17S–T aluminum-alloy plates with freely supported edges (average over 1-in. gage length).

against the pressure in figure 21. The strains across the diagonals at the corners are seen to increase rapidly above the strains at the center of the plate as the strain exceeds 0.001. The slope of the strain-pressure curve for the corners of the two thinner plates increased sharply for strains of 0.004 to 0.005, indicating yielding of the plate material.

The washboarding pressures p_y, $p_{2a/200}$, and $p_{2a/500}$ are indicated in figures 18 and 20 to facilitate comparison with the measured strains. The surface strains at the center of the plates with clamped edges (figs. 18 and 20) were less than 0.0025 at the washboarding pressures. Since this value is below the strain for which the material begins to yield (see fig. 1), washboarding could not be ascribed to yielding at the center. In the case of the plates with freely supported edges (see fig. 21), the strains across the diagonals at the corners were above the elastic region at the washboarding pressures (table 4) while they were well within the elastic range at the center. Washboarding, in these plates with freely supported edges, was therefore probably due to the formation of diagonal folds at the corners. This fact is brought out further by a comparison of the bending strains shown in figure 22, which were derived from the change in contour of plate 54 having freely supported edges corresponding to an increase in pressure from 1 to 15 pounds per square inch. The bending strains across the diagonals near the corner were considerably larger than the strains elsewhere in the plate.

Washboarding of the plates with clamped edges was ascribed to yielding along the edges due to the clamping stresses. In order to verify this result experimentally, slots parallel to the edges were cut in plate 31 after it had washboarded severely as a result of a normal-pressure test. The slots relieved the residual stresses due to bending along the edges and caused the inner portion of the plate to flatten so that the permanent set

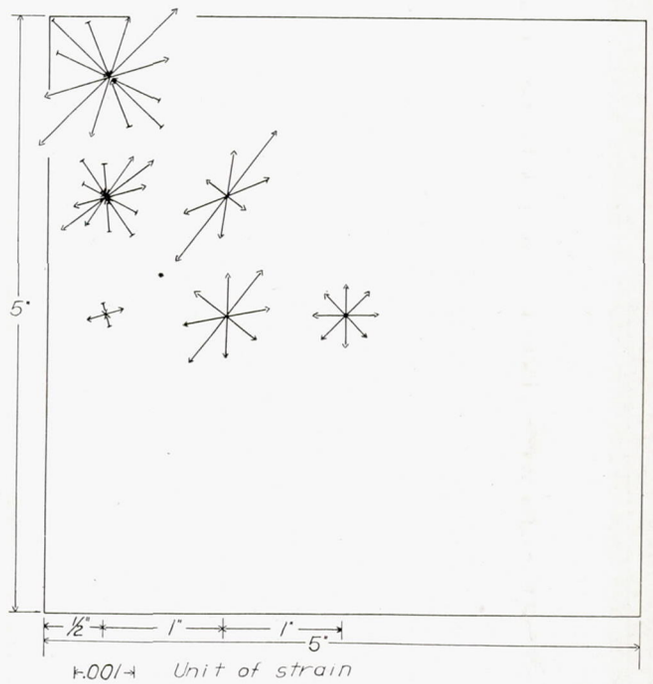

FIGURE 22.—Bending strains from contours on top of 5- by 5-inch 17S–T aluminum-alloy plate 54 with freely supported edges. Strains correspond to change in pressure between 1 and 15 pounds per square inch.

at the center of the plate was reduced from 0.22 to 0.04 inch. It was concluded that the washboarding in this plate was principally due to local bending stresses caused by clamping along the edges.

The direction of the principal strains at the surface of a 2.5- by 7.5-inch plate with clamped edges was obtained by observing the crack pattern in a coating of Run Kauri varnish dissolved in turpentine. The coating was applied and was allowed to dry before the plates were mounted in the fixture. Preliminary tests of such coatings had shown that they formed cracks normal to the direction of principal tensile strain when this strain attained a critical value that ranged from 10^{-3} to 2×10^{-3} depending on humidity, temperature, thickness of coating, and other factors. The cracks in a given region of

the plate were plainly visible when viewed from the proper angle, but it was impossible to photograph them because of the double curvature of the plate. A sketch of the pattern on both the top face of the plate and the bottom face of the plate is given in figure 23.

The crack pattern shows that the effect of the ends did not extend beyond a distance of about one span length into the plate; this result agrees with the conclusion obtained from the deflection curve (fig. 10). The clamping moment due to bending produced a band of parallel cracks on the bottom (pressure) face of the plate. The inflection marking the reversal in sign of the bending strain occurred at a distance from the center of about $0.72a$, which is considerably more than the distance of $0.58a$ for a beam with clamped ends under uniformly distributed load.

ANALYSIS

DEFLECTION

The contour of a rectangular plate subjected to normal pressure will have a fixed shape (that is, deflections at a given point will be a fixed percentage of the deflection at the center) only at pressures that are low enough to make the membrane stresses negligible compared with the bending stresses. The contour along a principal axis of a square plate as derived by Nádai (reference 6, pp. 180–184, equation (18)) for small deflections and as derived by Levy (reference 7) for $w_0/h=1.9$ are given in figure 8. The contour for small deflections resembles the deflection curve of a beam with clamped ends under a uniformly distributed load, but it has an inflection point at a distance from the center of $0.64a$ as compared with $0.58a$ for the beam.

As the center deflection of the rectangular plate increases under increasing normal pressure, catenary tensions become appreciable and the contour gradually approaches that for a square membrane. The theoretical deflection of a square membrane along its principal axes is not known exactly, but this deflection curve is likely to be nearly parabolic in shape, in view of the analogy with the circular membrane (equation (6) of reference 5).

This result is also supported by Boobnov's solution (reference 12) for an infinite strip of constant span rigidly clamped at the edges and subjected to uniform pressure. The transverse deflection curve at very low pressures has the shape

$$\frac{w}{w_0}=\left[1-\left(\frac{x}{a}\right)^2\right]^2 \tag{1}$$

characteristic of a beam with clamped ends under uniformly distributed load and of a circular plate with clamped edges under uniform pressure (reference 5), while at high pressures the plate strip deflects into a portion of a circular cylinder approached by the parabola

$$\frac{w}{w_0}=1-\left(\frac{x}{a}\right)^2 \tag{2}$$

The deflection curves from equations (1) and (2) are also given in figure 8. The measured deflection curves for clamped square plates were between the two types, approaching equation (2) as the pressure increased.

In the case of a simply supported square plate, the shape of the deflection curve for very low pressures ($w_0/h<<1$) as derived by Navier (see reference 6, p. 118, equation (25)) and shown in figure 9 differs only slightly from that for a plate with $w_0/h=2.47$ as derived by Kaiser (reference 8), which is also shown in figure 9. The shape of the observed deflection curve agrees with the theoretical curves within the error of measurement.

An "exact" curve of center deflection against pressure for a square plate with clamped edges as obtained by Levy (reference 7) and approximate curves of center

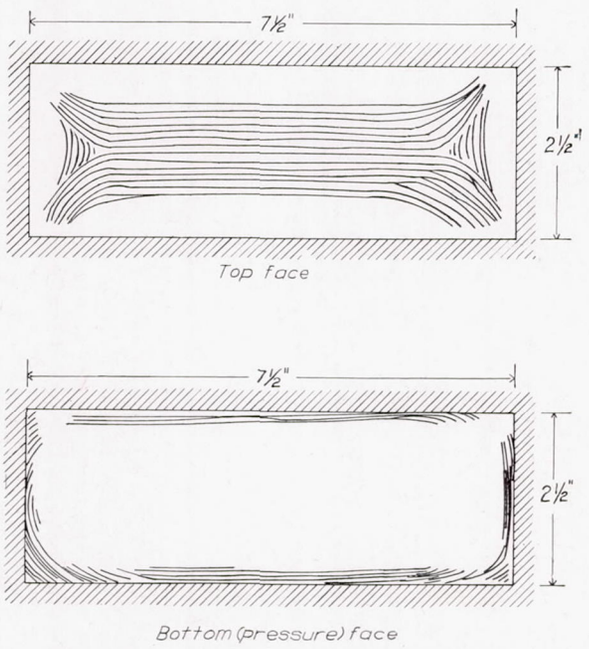

FIGURE 23.—Pattern of cracks in coating of Run Kauri on plate 24 after pressure of 100 pounds per square inch. Cracks are normal to largest principal tensile strain on surface.

deflection against pressure for plates with clamped edges having span-length ratios $a/b=1$, $\frac{2}{3}$, $\frac{1}{2}$ as obtained by Way (reference 11) are given in figure 24. An approximate curve for clamped square plates derived on the basis of the assumption in reference 13 of setting the total pressure equal to the sum of the pressures that would independently be resisted in tension and in bending

$$\frac{w_0}{h}+0.411\left(\frac{w_0}{h}\right)^3=0.224\,\frac{p}{E}\left(\frac{a}{h}\right)^4 \tag{3}$$

and an exact curve for a plate of infinite length due to Boobnov (reference 12) are also given in figure 24. It should be noted, in this connection, that Boobnov's work was extended for this purpose from $w_0/h=1.8$ to $w_0/h=13$ and that the effect of Poisson's ratio μ was included. Part of the extension of Boobnov's work up to values of $w_0/h=4.3$ was done by Way (see ch. 1

of reference 9); the rest of the extension up to $w_0/h=13$ was done by the authors of this paper. Way (reference 11) did not carry his calculations for a rectangular plate beyond $w_0/h=2$ because the degree of approximation became rapidly worse for center deflections of this order. It appears, however, from the curves in the lower portion of figure 24 that Way's approximate curve for $a/b=1$ (square plate) agrees closely with Levy's "exact" curve and with Föppl's still more approximate formula (3); whereas, Way's curve for $a/b=\frac{1}{2}$ agrees closely with Boobnov's solution for $a/b=0$, thus confirming the previous conclusion that a clamped-edge plate having a length of twice its span deflects substantially as a plate of infinite length.

It was felt, in view of the foregoing comparisons, that Way's, Boobnov's, and Föppl's theories would form a satisfactory basis for rating the clamped-edge plate with respect to the degree with which the theoretical clamping conditions were satisfied. This rating was done by comparing the observed center deflection against pressure curve with the appropriate theoretical curve, specifically by deriving the following deviation indices:

$$\frac{\Delta w_0}{w_{00}}=\frac{w_0-w_{00}}{w_{00}} \tag{4}$$

where w_0 and w_{00} are the observed and the theoretical center deflections, respectively.

The choice of w_{00} was governed by the scatter of points on the observed center deflection against pressure curves; w_{00} was chosen as small as possible consistent with the requirement that the corresponding observed center deflection w_0 could be accurately determined from the observations.

The deviation indices $\Delta w_0/w_{00}$, as well as the definition upon which they were derived in the individual cases, are given in table 3 for all the plates with clamped edges. The deviation index was less than 0.2 for only 21 of the 56 plates tested. It exceeded 0.5 for 15 of the plates. It may be concluded that the theoretical clamping conditions were approximated for only a fraction of the plates tested. The center deflections for a 17S–T aluminum-alloy plate and a stainless-steel plate with deviation indices of less than 1 percent are plotted in figure 24 for comparison with the calculated values. Calculated and observed deflections check within 5 percent for the aluminum-alloy plate 8 up to $w_0/h=12$. The deflection of the stainless-steel plate exceeded the theoretical deflection except at very low pressures by an amount that increased with the pressure. This variation was ascribed to the peculiar stress-strain curve of the material. (See fig. 2.)

Kaiser (reference 8) has computed the contour and the stress distribution for a plate with freely supported edges under a normal pressure producing a center deflection $w_0=2.47h$. Kaiser was able to check his theoretical value against empirical curves obtained from experiments on a 600- by 600- by 3.15-millimeter (23.6- by 23.6- by 0.124-in.) steel plate. Kaiser's empirical curve

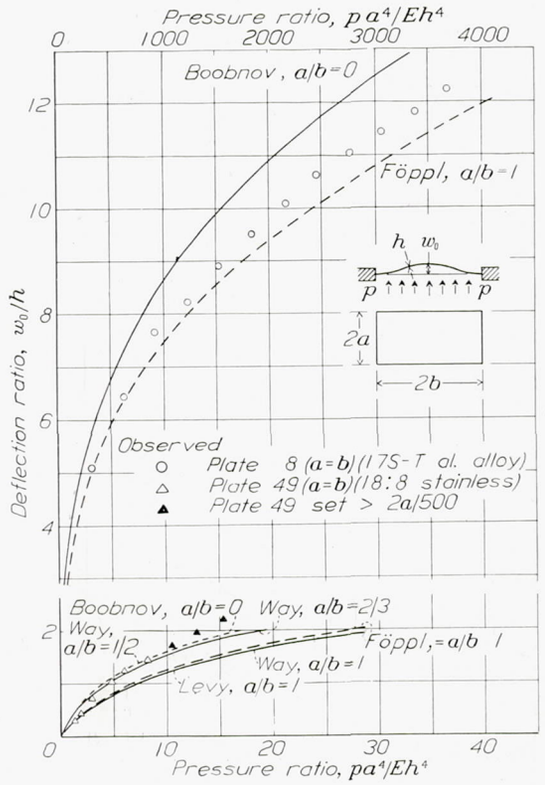

FIGURE 24.—Center deflection against pressure for rectangular plates with clamped edges. Poisson's ratio, 0.3.

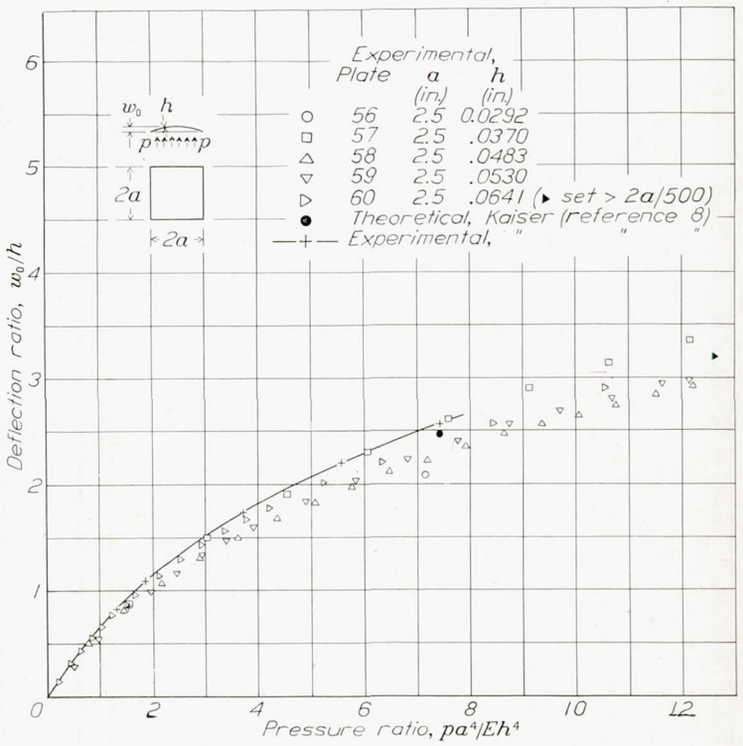

FIGURE 25.—Center deflection against pressure for freely supported square plates. Poisson's ratio, 0.3.

and theoretical point are compared with the observed center deflections for the five plates tested with supported edges in figure 25. The observed deflections differed less than 20 percent from Kaiser's values. The deviation indices $\Delta w_0/w_{00}$ are given in table 4. They ranged from 0.00 to −0.20. This variation indicates some restraint at the edges that would cause a reduction in the center deflection.

STRESSES

The only exact solutions for the stresses in a rectangular plate of medium thickness with clamped edges known to the authors are the ones derived by Boobnov (reference 12) for the asymptotic case of the plate strip of infinite length and by Levy (reference 7) for a square plate. Probably the best approximate solution for the stresses in a rectangular plate is that due to Way (reference 11).

The solution for a plate strip of infinite length differs from that for the square plate in that the median-fiber tension becomes uniform across the strip in the plate

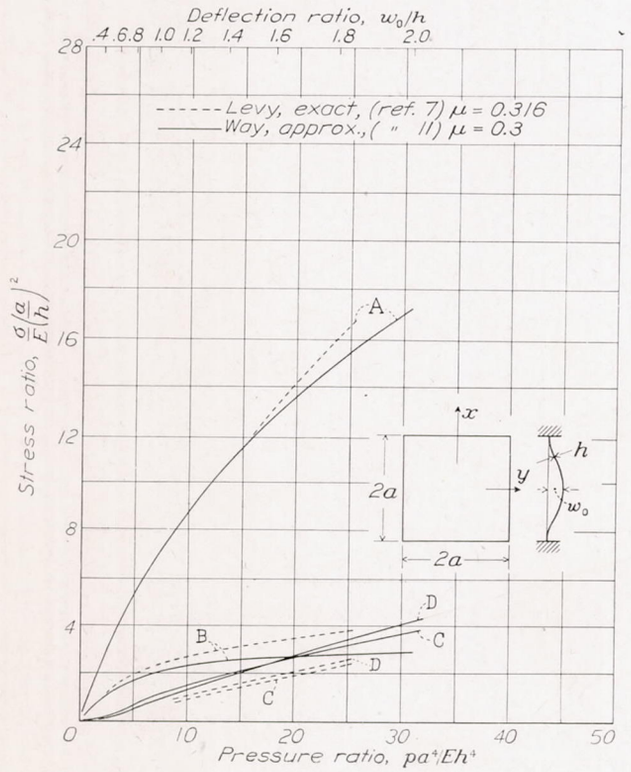

FIGURE 26.—Stress in a square plate with clamped edges.

A, $\frac{\sigma''_{xe}}{E}\left(\frac{a}{h}\right)^2$; B, $\frac{\sigma''_{xo}}{E}\left(\frac{a}{h}\right)^2$; C, $\frac{\sigma'_{xe}}{E}\left(\frac{a}{h}\right)^2$; D, $\frac{\sigma_{xo}}{E}\left(\frac{a}{h}\right)^2$.

strip instead of being greater at the center than at the edges as in the square plate. The median-fiber stresses and the extreme-fiber bending stresses at the center of the plate and at the midpoint of the longer edge are plotted against the pressure in dimensionless form for plates of finite dimensions ($a/b = 1$ and 2/3) in figures 26 and 27 and for a plate strip ($a/b = 0$) in figure 28 where the new symbols on the figures have the following significance:

σ''_{xo} extreme-fiber bending stress at center
σ''_{xe} extreme-fiber bending stress at midpoint of edge
σ'_{xo} median-fiber tensile stress at center
σ'_{xe} median-fiber tensile stress at midpoint of edge

In figures 27 and 29 subscript xe indicates the midpoint of the longer edge. The median-fiber stresses and the extreme-fiber bending stresses at the point of maximum stress—the center of the longest edge—are plotted against the pressure in dimensionless form for a plate

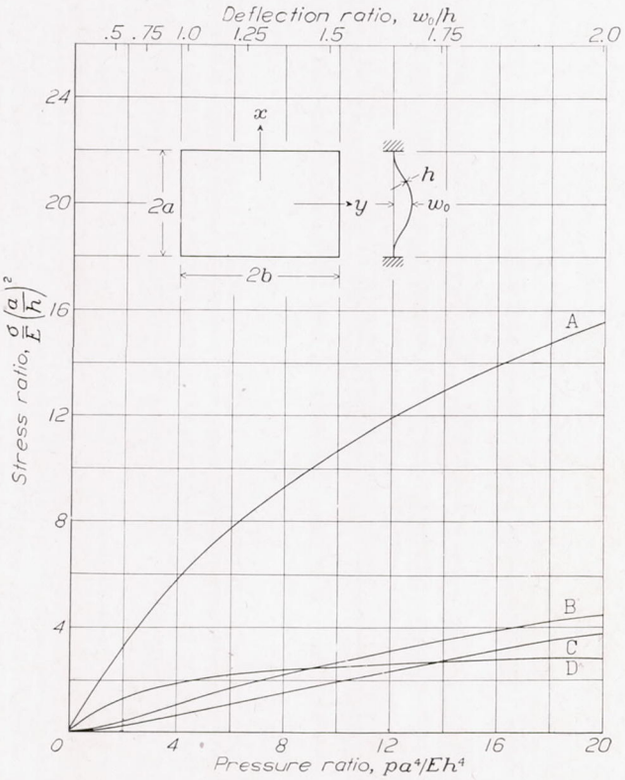

FIGURE 27.—Stress in a rectangular plate ($a/b = 2/3$) with clamped edges according to reference 11. Poisson's ratio, 0.3.

A, $\frac{\sigma''_{xe}}{E}\left(\frac{a}{h}\right)^2$; B, $\frac{\sigma'_{xe}}{E}\left(\frac{a}{h}\right)^2$; C, $\frac{\sigma'_{xo}}{E}\left(\frac{a}{h}\right)^2$; D, $\frac{\sigma''_{xo}}{E}\left(\frac{a}{h}\right)^2$.

with $a/b = 1/2$ in figure 29. Approximate values of the center deflection ratio w_0/h are given on the abscissa scale to show the effect of center deflection on the median-fiber stresses.

The resultant extreme-fiber stresses at the center of the plate and at the midpoint of the longer edge were obtained from figures 26 to 29 by adding the extreme-fiber stress and the median-fiber stress and are shown in figure 30. The extreme-fiber stress at the midpoint of the longer edge is from 2 to 4 times as great as that at the center of the plate. Yielding due to bending along the edges should therefore always precede yielding due to tension at the center in an ideally clamped plate. Although Way's solution for the square plate $a/b = 1$ agrees well with the exact solution by Levy, the approximate nature of Way's solution must be kept in mind in comparing the stresses in the rectangular plate with those in the infinite plate as given in figure 30. As Way points out (reference 11) his curves indicate that,

at the midpoint of the longer edge of a finite plate with $a/b=2/3$ or less, a greater stress is caused by a given pressure than in an infinite-plate strip of the same material and the same cross-sectional dimensions. This result is, of course, incorrect and it may be ascribed to the approximate nature of Way's solution.

The theoretical strain ϵ at the center of the square plate may be derived from references 7 and 11 by substitution in

$$\epsilon=(1-\mu)\sigma/E \tag{5}$$

where σ is the stress and μ is Poisson's ratio. The resulting curves of extreme-fiber strain against pressure are shown dashed in figures 16, 19, and 20 for comparison with the measured extreme-fiber strain over a 1-inch gage length. There is approximate agreement in

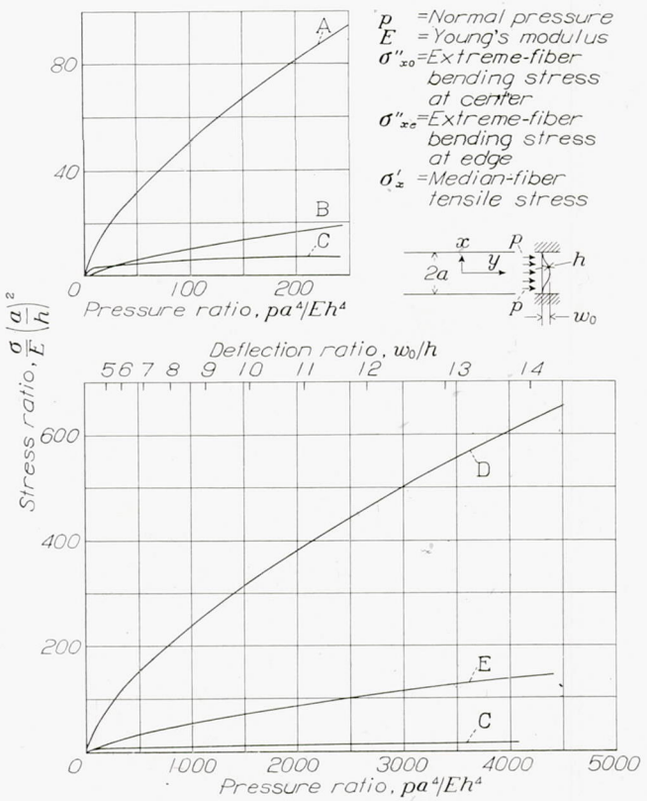

FIGURE 28.—Stress in infinite plate strip ($a/b=0$) with clamped edges according to reference 12. Poisson's ratio, 0.3.

A, $\frac{\sigma''_{x_0}}{E}\left(\frac{a}{h}\right)^2$; B, $\frac{\sigma'_x}{E}\left(\frac{a}{h}\right)^2$; C, $\frac{\sigma''_{x_0}}{E}\left(\frac{a}{h}\right)^2$; D, $\frac{\sigma''_{x_e}}{E}\left(\frac{a}{h}\right)^2$; E, $\frac{\sigma'_x}{E}\left(\frac{a}{h}\right)^2$.

the case of figures 19 and 20 but the theoretical strains are about 30 percent higher than the measured strains in the case of figure 16.

The stress distribution in a square plate of medium thickness with freely supported edges has been investigated both theoretically and experimentally with great thoroughness by Kaiser (reference 8). Figure 31 shows the extreme-fiber bending stress σ'' and the median-fiber tensile stress σ' according to Kaiser for gage lines at the center of the plate, parallel to the edge of the plate, and across the diagonal at a point near the corners for which the coordinates relative to the center were $x/a=y/a=0.6$. The last gage line is included because Kaiser's work showed that it marked the region of maximum bending stress for plates in which the center deflection was comparable with the plate thickness.

Figure 32 shows the extreme-fiber stress σ obtained by adding the bending stress to the median-fiber stress as given in figure 31. Comparison of figure 32 with figure 30 shows that, for the pressure ratios investigated,

$$\frac{pa^4}{Eh^4}<8$$

the square plate with rigidly clamped edges supports approximately the same normal pressure at a given maximum extreme-fiber stress as a plate of the same dimensions and material with freely supported edges.

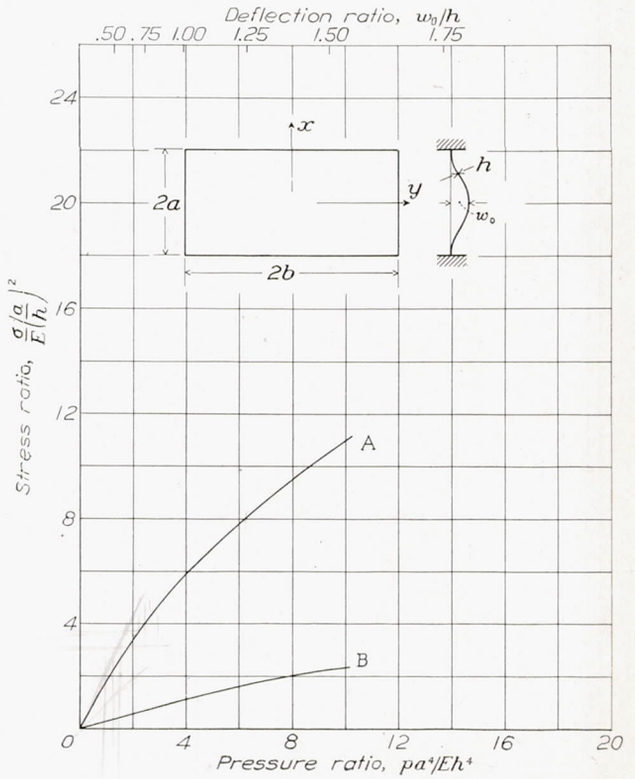

FIGURE 29.—Stress in a rectangular plate ($a/b=1/2$) with clamped edges according to reference 11. Poisson's ratio, 0.3.

A, $\frac{\sigma''_{x_e}}{E}\left(\frac{a}{h}\right)^2$; B, $\frac{\sigma'_{x_e}}{E}\left(\frac{a}{h}\right)^2$.

Extreme-fiber bending strains ϵ were measured in the plates with supported edges at the center and across the diagonal at $x/a=y/a=0.83$. These strains are compared on a dimensionless basis in figure 33 with the extreme-fiber bending strains obtained from Kaiser's theoretical and experimental stresses (reference 8) along mutually perpendicular directions by substitution in the equation

$$\epsilon_x=(\sigma_x-\mu\sigma_y)/E \tag{6}$$

The measured strains agree with Kaiser's theoretical and experimental values within the scatter in the present tests.

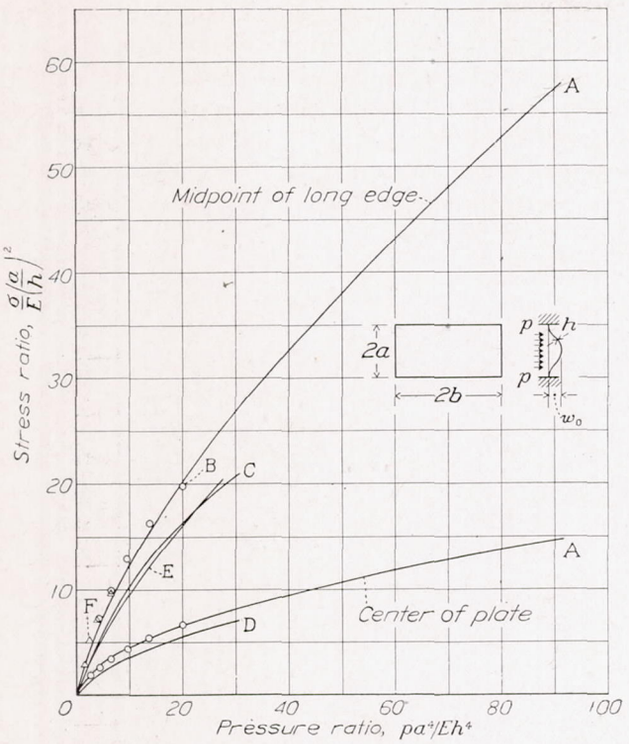

FIGURE 30.—Extreme-fiber stresses for rectangular plates with clamped edges. σ, stress; E, Young's modulus. A, $\frac{a}{b}=0$, Boobnov (reference 12); B, $\frac{a}{b}=\frac{2}{3}$, Way (reference 11); C, $\frac{a}{b}=1$, Way (reference 11); D, $\frac{a}{b}=1$, Levy and Way (references 7 and 11); E, $\frac{a}{b}=1$, Levy (reference 7); F, $\frac{a}{b}=\frac{1}{2}$, Way (reference 11).

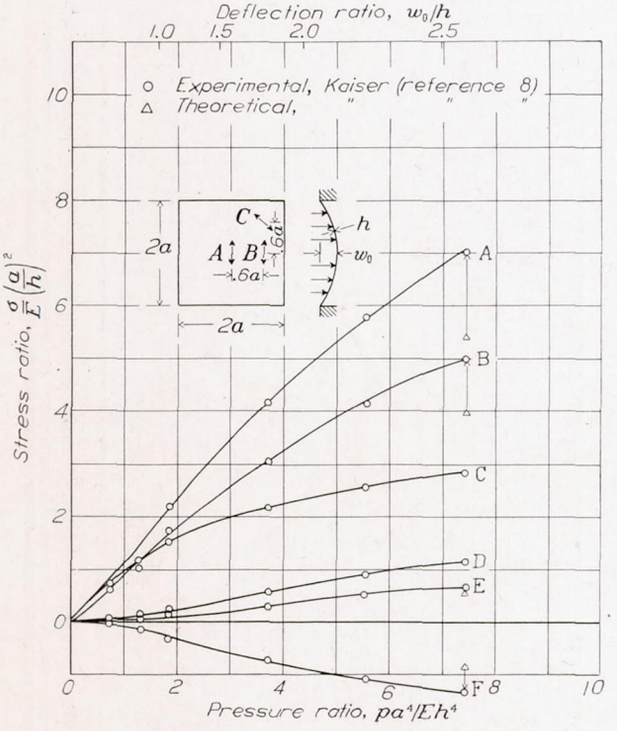

FIGURE 31.—Stresses in a square plate with freely supported edges according to reference 8. Poisson's ratio, 0.3. p, normal pressure; E, Young's modulus; σ'' bending stress; σ', median-fiber stress.

A, $\frac{\sigma''C}{E}\left(\frac{a}{h}\right)^2$; B, $\frac{\sigma''B}{E}\left(\frac{a}{h}\right)^2$; C, $\frac{\sigma''A}{E}\left(\frac{a}{h}\right)^2$; D, $\frac{\sigma'A}{E}\left(\frac{a}{h}\right)^2$; E, $\frac{\sigma'B}{E}\left(\frac{a}{h}\right)^2$; F, $\frac{\sigma'C}{E}\left(\frac{a}{h}\right)^2$.

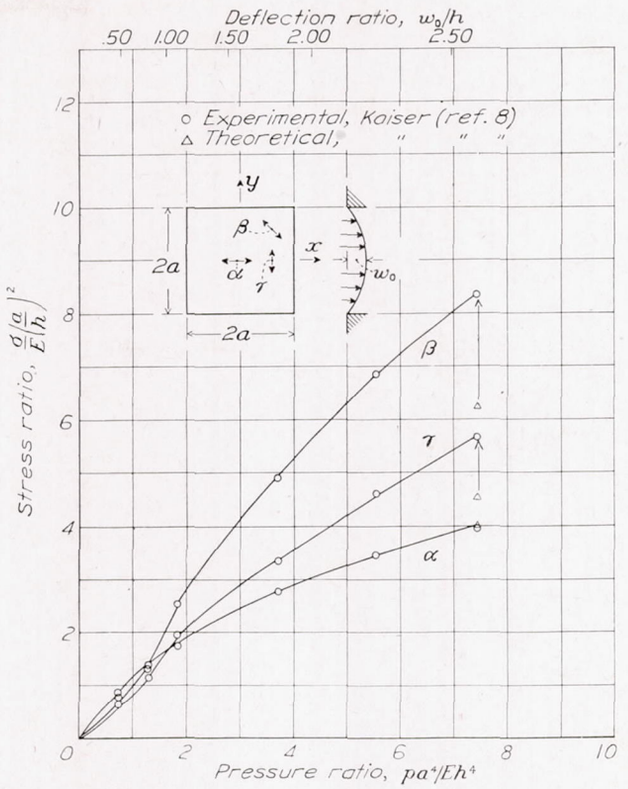

FIGURE 32.—Maximum extreme-fiber stresses in a square plate with freely supported edges according to reference 8. Poisson's ratio, 0.3. β, across diagonal at $\frac{x}{a}=\frac{y}{a}=0.6$; γ, along axis $\frac{x}{a}=0.6$, $\frac{y}{a}=0$; α, along axis $\frac{x}{a}=\frac{y}{a}=0$.

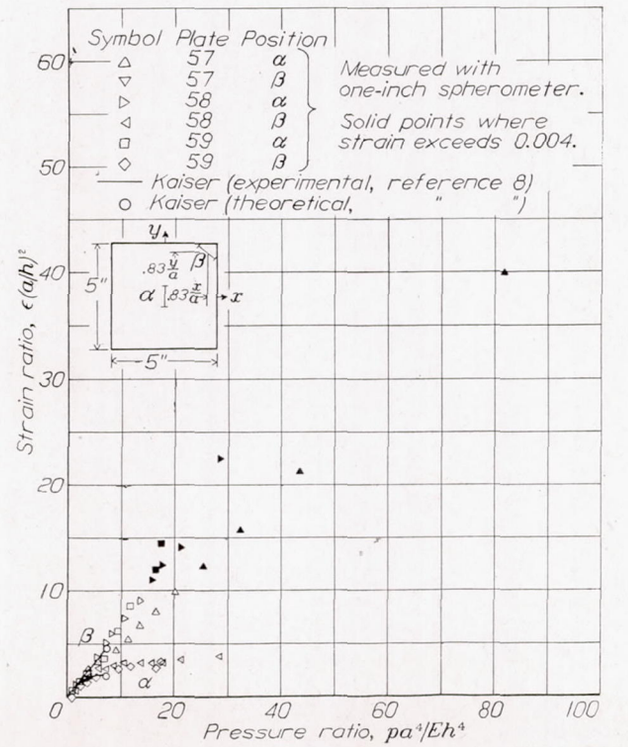

FIGURE 33.—Bending strain in a square plate with freely supported edges.

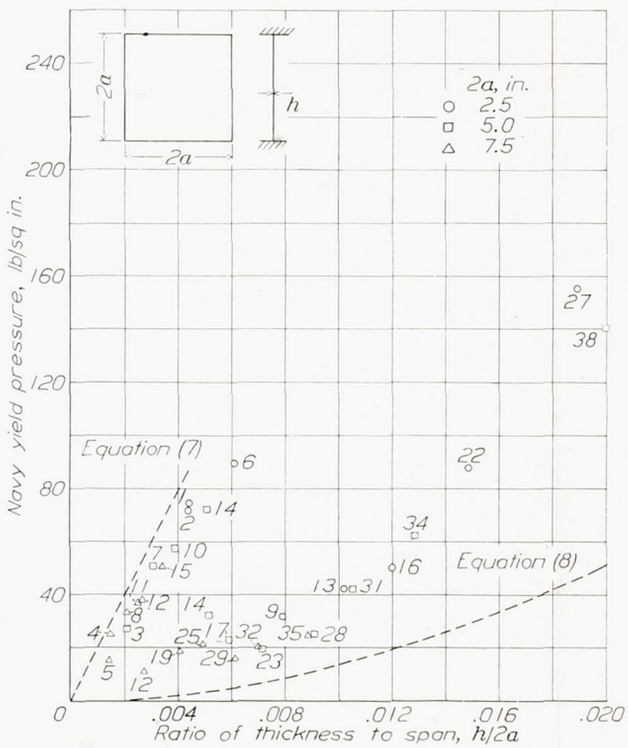

FIGURE 34.—Washboarding pressures (Navy yield pressure) for square 178–T aluminum-alloy plates with clamped edges. Plates 12 and 14 had two distinct yield pressures.

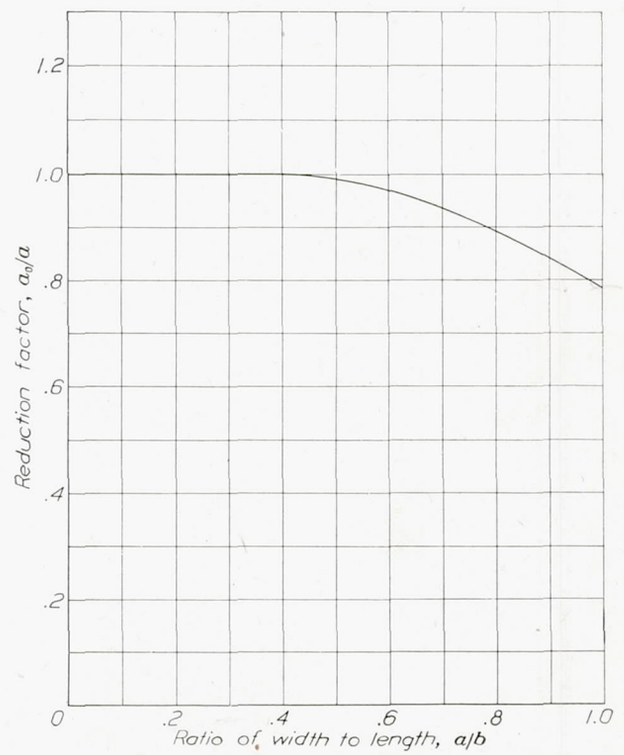

FIGURE 35.—Reduction factor for maximum stress at center of longest side of clamped rectangular plates. $2a$, actual span; $2b$, actual length; $2a_0$, span of infinite plate strip having same stress at center of longest edge.

PERMANENT SET

Analysis of the washboarding pressures listed in table 3 indicated that the washboarding of the square plates with clamped edges was brought about by two manners of failure. Very thin plates, that is, plates with negligible flexural rigidity, will carry practically all of the load as a membrane and they may be expected to fail by yielding throughout the plate like a membrane. If the plate remains elastic up to the yield point, the relation between pressure p_y and stress σ_y at the center of the plate may be approximated by the following formula (see reference 13, p. 230)

$$p_y=8.0E\left(\frac{h}{2a}\right)\left(\frac{\sigma_y}{E}\right)^{3/2} \tag{7}$$

that is, the washboarding pressure should vary directly with the ratio of thickness to span $h/2a$.

Relatively thick plates, that is, plates in which practically all of the load is carried by bending and almost none by membrane action, will yield owing to the local bending stresses at the center of the clamped edges. If

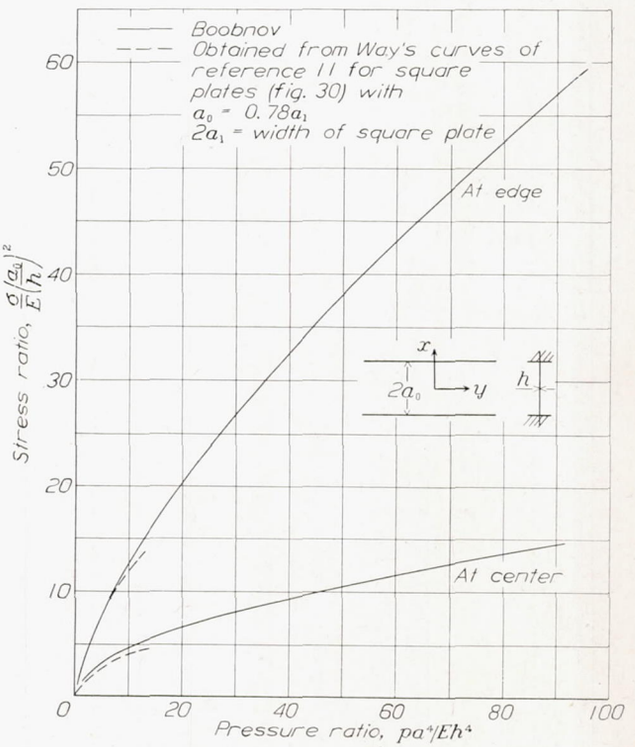

FIGURE 36.—Extreme-fiber stress in infinite plate strip ($a/b=0$), clamped edges according to reference 12. Poisson's ratio, 0.3. p, pressure; E, Young's modulus.

the plate is rigidly clamped and remains elastic up to the beginning of yielding at this point, the pressure p_y corresponding to an extreme-fiber stress σ_y at the center of the edge is, according to reference 6 (p. 184),

$$p_y=3.2E\left(\frac{h}{2a}\right)^2\frac{\sigma_y}{E} \tag{8}$$

that is, the washboarding pressure varies directly with the square of the ratio of thickness to span $(h/2a)^2$.

Before these two mechanisms of failure are considered further, it should be noted that the highest stress in a perfectly clamped rectangular plate will always occur at the center of the longer pair of clamped edges. (See fig. 30.) Yielding at the edges should therefore precede

yielding in any other portion of the plate and hence only the second mechanism of failure seems admissible on theoretical grounds. Yielding due to membrane action may, nevertheless, be present in an actual and, therefore, an imperfectly clamped plate if either one of the following two factors is important:

1. The clamps may permit a sufficient angular rotation of the edge of the plate to remove a large portion of the local bending stress at the center of the edge.

2. The yield strength of the material when subjected to the local bending stress with a large gradient at the edge of the plate may be much higher than the yield strength under the more nearly uniform tension present in the rest of the plate.

The two types of failure characterized by equations (7) and (8) are brought out clearly in figure 34 by plotting p_y against $h/2a$ for the square 17S–T aluminum-alloy plates given in table 3. The washboarding pressure goes up linearly with $h/2a$ for values of $h/2a$ less than about 0.004. It goes up with the square of $h/2a$ for values of $h/2a$ greater than about 0.006. The approximate formulas (7) and (8) are plotted in figure 34 for comparison with the observed values, assuming the average values

$\sigma_y = 40{,}000$ pounds per square inch

$E = 10.3 \times 10^6$ pounds per square inch

The pressures from equation (7) are about 30 percent high for

$$\frac{h}{2a} < 0.0025$$

while those from equation (8) are about 60 percent low for

$$\frac{h}{2a} > 0.006$$

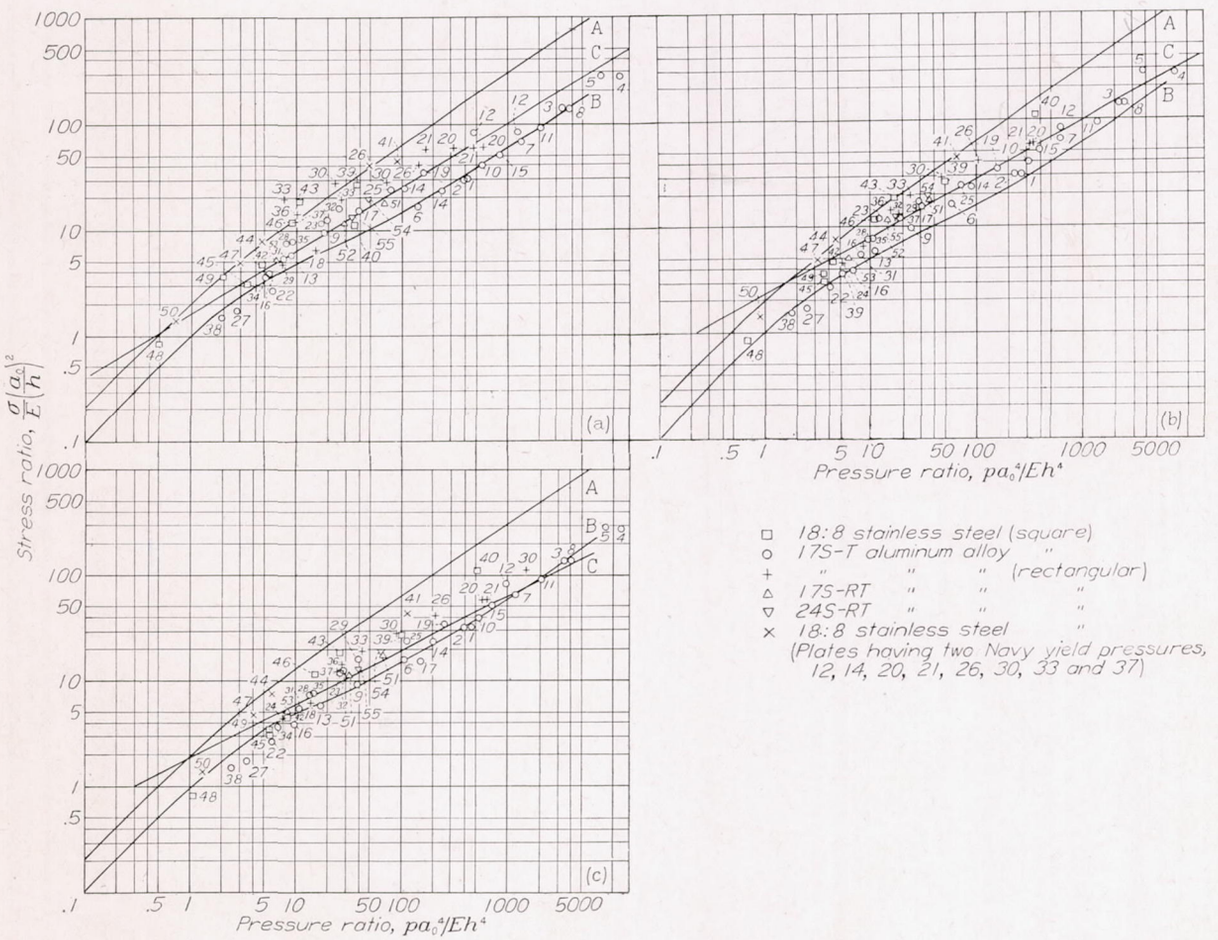

(a) Navy yield pressure p.
(b) Pressure p for set at center of $2a/500$.
(c) Pressure p for set at center of $2a/200$.

FIGURE 37.—Pressures for plates with clamped edges. σ_y, yield strength; E, Young's modulus; $2a$, span for equivalent plate strip; h, thickness; A, yielding at edge (Boobnov, reference 12); B, yielding at center (Boobnov, reference 12); C, empirical straight line.

The formulas (7) and (8) are useless in describing the washboarding of square clamped plates in the important intermediate range of $0.0025 < h/2a < 0.0060$ in which both the membrane stresses and the bending stresses seem to take an appreciable share of the load. Inclusion of this intermediate range in the analysis of washboarding pressures requires a consideration of stresses in plates of intermediate thickness as derived by Levy, Way, and Boobnov. (See references 7, 11,

and 12.) It was assumed for the purpose of such an analysis that washboarding would be associated with yielding either along the edge of the plate or at the center of the plate and that this yielding would take place when the theoretical stress at these two points attained a stress σ_y at which the material begins to yield in tension. The results of this assumption differ from those made upon assumption of the von Mises-Hencky theory of failure (reference 5) only for the stress σ_{xo} at the center of a square plate and there the difference in stress is only 11 percent. The same results are obtained from both assumptions for the theoretical stress σ_{xe} for yielding along the edge of any plate and the stress σ_{xo} for yielding at the center of an infinite-plate strip.

For rectangular plates the relation between the stresses σ_{xe} and σ_{xo} and the pressure p is given in figures 26 and 27 by the dimensionless plots of $\frac{\sigma_{xe}}{E}\left(\frac{a}{h}\right)^2$ and $\frac{\sigma_{xo}}{E}\left(\frac{a}{h}\right)^2$ as functions of $\frac{p}{E}\frac{a^4}{h^4}$. Unfortunately, the value of these functions has been calculated only for $\frac{p}{E}\frac{a^4}{h^4}<31.2$ as compared with measured values for plate 4 that go up to 20,000. The only known theoretical solution for pressure ratios of this order is Boobnov's solution (reference 12) for the flat-plate strip with clamped edges. Figure 28 shows the extreme-fiber stresses at the edge and at the center of such a strip up to values of $\frac{p}{E}\frac{a^4}{h^4}=4500$.

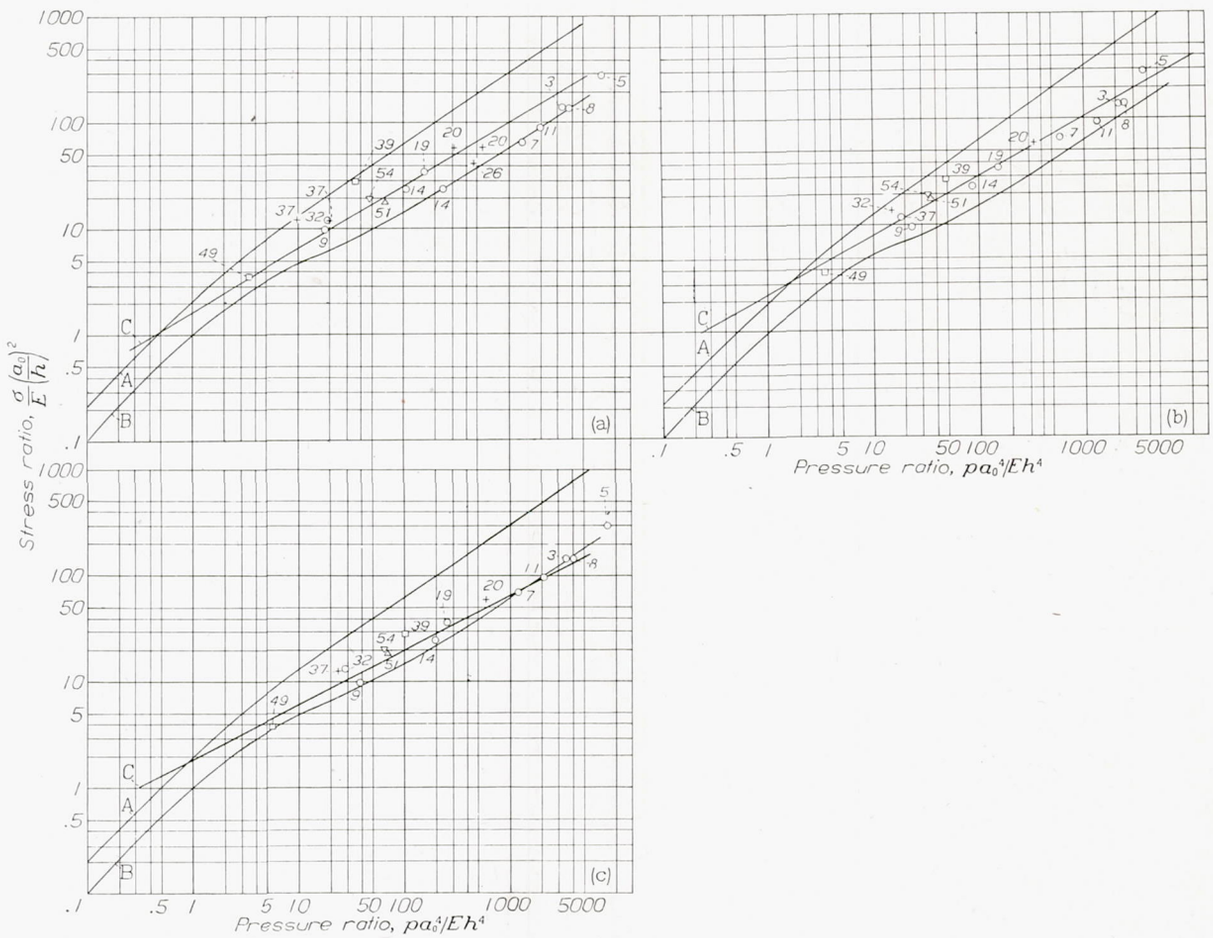

(a) Navy yield pressure p.
(b) Pressure p for set at center of $2a/500$.
(c) Pressure p for set at center of $2a/200$.

FIGURE 38.—Pressures for plates with clamped edges.

$(-0.1<\frac{\Delta w_o}{w_{oo}}<0.1)$. A, yielding at edge (Boobnov, reference 12); B, yielding at center (Boobnov, reference 12); C, empirical straight line.

A comparison of the experimental data on plates of finite length with Boobnov's theory for infinitely long plates was obtained by regarding the actual plate with a span $2a$ as an infinite plate of which the span $2a_0$ was less than that of the actual plate in order to allow for the strengthening effect of clamping at the short edges. The ratio a_0/a was arbitrarily chosen so that the initial slopes of the two curves for extreme-fiber bending stresses σ_{xe}'' at the center of the edge are brought into coincidence.

In the case of a square plate with clamped edges the

extreme-fiber bending stress at the center of the edge is, for low pressures (see reference 6, p. 184),

$$\sigma''_{xe}=1.22p\left(\frac{a}{h}\right)^2$$

while at the edge of a clamped plate strip of span $2a_0$ it is

$$\sigma''_{xe}=2p\left(\frac{a_0}{h}\right)^2$$

For identity of initial slope σ''_{xe}/p therefore,

$$a_0/a=\sqrt{1.22/2}=0.78$$

where

$2a$ actual span

$2a_o$ span of infinite-plate strip having same stress at midpoint of longer edge

The corresponding reduction factor for any rectangular plates with clamped edges ($0<a/b<1$) may be obtained by analogy from figure 113 (p. 184) of reference 6 with the result shown in figure 35. Application of this reduction factor to the curves for the extreme-fiber stresses at the center of the edge and at the center of a square plate in figure 30 leads to the dashed curves shown in figure 36. The extreme-fiber stresses for the equivalent plate strip are seen to differ less than 13 percent from the exact values. This method of reducing to an equivalent plate strip was accordingly used in comparing the observed washboarding pressures for rectangular plates with the theoretical values for an infinite plate.

The theoretical washboarding pressures for yielding at the edge and yielding at the center are shown as curves A and B, respectively, in figure 37, where $2a_0$ is the span for the equivalent plate strip (fig. 35). Log-log paper was chosen as in the case of the corresponding plots for the circular plates (figs. 28 to 30 of reference 5) in order to spread the observed values more uniformly over the sheet. The experimental washboarding pressures given in table 3 were plotted in figure 37 by replacing σ_y, the stress at which yielding begins in tension, by the average yield strength in a longitudinal direction and a transverse direction (table 1). The pressure for the beginning of yielding was replaced by the Navy yield pressure in figure 37(a), the pressure for a set at the center of 1/500 the span in figure 37(b), and the pressure for a set at the center of 1/200 the span in figure 37(c).

The measured Navy yield pressures and the pressures for a set of 1/500 the span were between the theoretical pressures for yielding at the edge and for yielding at the center for more than 80 percent of the plates. The pressures for a set of 1/200 the span were in approximate agreement with the theoretical pressure for yielding at the center of the plate. The scatter of the points is large, particularly in figure 37 (a). Part of this scatter could be ascribed to deviations from the theoretical clamping conditions because the scatter of the points with deviation indices between 0.1 and −0.1, which are shown in figure 38, was only about one-third as large as that for the entire array of points.

It is interesting to note that the measured washboarding pressures for very thin plates (in the right-hand portion of the figures) approached the theoretical curve for yielding at the center in every case. Very thin plates seemed to yield consistently like a thin membrane.

Straight lines C were fitted by the method of least squares to the observed washboarding pressures in figure 37. These lines are also shown in figure 38. The deviation of individual points from the lines C is large in many cases. Nevertheless, the lines may be useful in arriving at a rough estimate of washboarding pressure

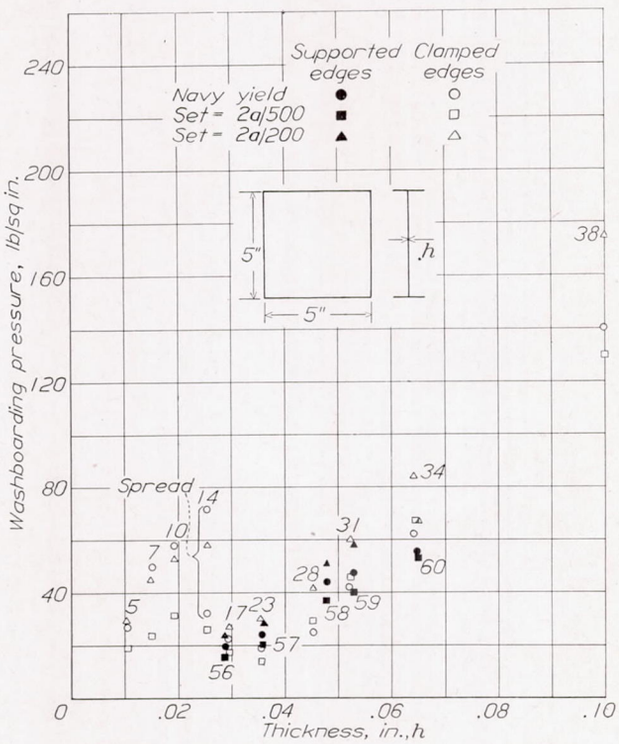

FIGURE 39.—Comparison of washboarding pressures for 5- by 5-inch 17S–T aluminum-alloy plates.

for a rigidly clamped plate of given dimensions and given material.

In the case of plates with freely supported edges, an adequate theory for the stress distribution at sufficiently high values of the deflection ($w_0/h=10$) was not available. Kaiser's theory (reference 8) goes up only to $w_0/h=2.7$. Inasmuch as only five square plates of only one size (5- by 5-in.) and one material (17S–T aluminum alloy) were tested, the empirical data were insufficient either to check any proposed theory or to provide empirical relations of any generality. The washboarding pressures are compared with the washboarding pressures of 5- by 5-inch 17S–T aluminum-alloy plates with clamped edges in figure 39. The washboarding pressures for the plates with freely supported

edges were approximately the same as those for the clamped-edge plates. The reason for this approximate agreement may be that, in the case of the plates with freely supported edges, the diagonal folds in the corners caused nearly as high bending stresses as were observed at the midpoint of the longer edges of the plates with clamped edges.

NATIONAL BUREAU OF STANDARDS,
WASHINGTON, D. C., *November 28, 1941.*

REFERENCES

1. The William Froude National Tank and the Marine and Armament Experimental Establishment: P.5 Flying Boat N. 86, Impact Tests—(Experiments with Full Size Machines. Third Series). R. & M. No. 926, British A. R. C., 1924.
2. Baker, G. S., and Keary, E. M.: Experiments with Full-Sized Machines. Second Series. R. &. M. No. 683, British A. R. C., 1920.
3. Wagner, Herbert: Landing of Seaplanes. T. M. No. 622, NACA, 1931.
4. Mesnager, A.: Calcul Elementaire rigoureux des plaques rectangulaires. Int. Assoc. for Bridge and Structural Eng., 1932, pp. 329–336.
5. McPherson, Albert E., Ramberg, Walter, and Levy, Samuel: Normal-Pressure Tests of Circular Plates with Clamped Edges. Report No. 744, NACA, 1942.
6. Nádai, A.: Elastische Platten. Julius Springer (Berlin), 1925.
7. Levy, Samuel: Square Plate with Clamped Edges under Normal Pressure Producing Large Deflections. Rep. No. 740, NACA, 1942.
8. Kaiser, Rudolf: Rechnerische und experimentelle Ermittlung der Durchbiegungen und Spannungen von quadratischen Platten bei freier Auflagerung an den Rändern, gleighmässig verteilter Last unter grossen Ausbiegungen. Z. f. a. M. M., Bd. 16, Heft 2, April 1936, pp. 73–98.
9. Timoshenko, S.: Theory of Plates and Shells. McGraw-Hill Book Co., Inc., 1940.
10. Ramberg, Walter, McPherson, Albert E., and Levy, Sam: Experimental Study of Deformation and of Effective Width in Axially Loaded Sheet-Stringer Panels. T. N. No. 684, NACA, 1939.
11. Way, Stewart: Uniformly Loaded, Clamped, Rectangular Plates with Large Deflection. Proc. Fifth Int. Cong. Appl. Mech. (Cambridge, Mass., 1938), John Wiley & Sons, Inc., 1939, pp. 123–128.
12. Boobnov, Ivan G.: On the Stresses in a Ship's Bottom Plating Due to Water Pressure. Trans. Inst. Naval Arch., vol. XLIV, 1902, pp. 15–52.
13. Föppl, Aug., and Föppl, Ludwig: Drang und Zwang. Vol. I., R. Oldenbourg (Munich), 2d ed., 1924.

TABLE 1.—DIMENSIONS FOR PLATES FOR CLAMPED-EDGE TESTS

Plate	Material [a]	Span, $2a$ (in.)	Length, $2b$ (in.)	Thickness, h (in.)	Young's modulus, E (kips/sq in.)	Tensile yield strength (kips/sq in.) (Offset=0.002)	
						Longitudinal	Transverse
1	A	2.5	2.5	0.0110	10,300	43.0	38.0
2		2.5	2.5	.0110	10,300	43.0	38.0
3		5	5	.0104	10,300	43.0	38.0
4		7.5	7.5	.0111	10,300	43.5	38.0
5		7.5	7.5	.0109	10,300	43.0	38.0
6		2.5	2.5	.0153	10,300	44.0	37.5
7		5	5	.0151	10,300	44.0	37.5
8		7.5	7.5	.0158	10,300	44.0	37.5
9		2.5	2.5	.0197	10,300	43.0	37.0
10		5	5	.0193	10,300	43.0	37.0
10a		5	5	.0202	10,300	43.0	37.0
11		7.5	7.5	.0191	10,300	43.0	37.0
12		7.5	7.5	.0200	10,300	43.0	37.0
13		2.5	2.5	.0255	10,400	44.0	37.5
14		5	5	.0255	10,400	44.0	37.5
15		7.5	7.5	.0256	10,400	44.0	37.5
16		2.5	2.5	.0300	10,200	39.5	35.0
17		5	5	.0297	10,200	39.5	35.0
18		2.5	7.5	.0303	10,200	38.1	36.5
19		7.5	7.5	.0302	10,200	38.1	35.5
20		7.5	17.5	.0295	10,200	39.5	35.0
21		7.5	17.5	.0301	10,200	38.5	35.5
22		2.5	2.5	.0371	10,200	40.8	36.5
23		5	5	.0357	10,200	42.4	37.5
24		2.5	7.5	.0369	10,200	42.4	38.0
25		7.5	7.5	.0373	10,200	42.5	36.5
26		7.5	17.5	.0375	10,200	42.5	37.5
27		2.5	2.5	.0474	10,300	46.5	38.6
28		5	5	.0455	10,300	45.8	38.6
29		7.5	7.5	.0460	10,300	44.6	38.6
30		7.5	17.5	.0450	10,300	44.6	38.6
31		5	5	.0526	10,400	46.0	37.9
32		7.5	7.5	.0527	10,400	43.0	37.9
33		7.5	17.5	.0529	10,400	43.0	37.9
34		5	5	.0653	10,300	43.7	37.0
35		7.5	7.5	.0663	10,300	42.0	37.5
36		7.5	17.5	.0634	10,300	43.2	38.0
37		7.5	17.5	.0668	10,300	42.0	37.5
38		5	5	.1000	10,300	44.2	[b] 37.4
39	B	2.5	2.5	.0127	29,000	133.0	140.0
40		5	5	.0127	29,000	133.0	140.0
41		2.5	7.5	.0127	29,000	133.0	140.0
42		2.5	2.5	.0281	28,500	104.0	118.0
43		5	5	.0283	28,500	104.0	118.0
44		2.5	7.5	.0281	28,500	104.0	118.0
45		2.5	2.5	.0339	28,000	104.0	99.0
46		5	5	.0342	28,000	104.0	99.0
47		2.5	7.5	.0340	28,000	104.0	99.0
48		2.5	2.5	.0597	28,000	90.0	90.0
49		5	5	.0590	28,000	90.0	90.0
50		2.5	7.5	.0601	28,000	90.0	90.0
51	C	2.5	7.5	.0208	10,300	53.9	48.2
52				.0254	10,300	52.3	46.9
53				.0384	10,300	54.2	46.6
54	D	2.5	7.5	.0204	10,300	54.1	50.2
55				.0250	10,300	[b] 54.1	[b] 50.2

[a] Material:
A is 17S–T aluminum alloy.
B is 18:8 stainless steel.
C is 17S–RT aluminum alloy.
D is 24S–RT aluminum alloy.
[b] Average for similar material tested.

TABLE 2.—PLATES WITH FREELY SUPPORTED EDGES—17S–T ALUMINUM ALLOY

Plate	Span, $2a$ (in.)	Length, $2b$ (in.)	Thickness, h (in.)	Young's modulus E (kips/sq in.)	Tensile yield strength (kips/sq in.) (Offset=0.002)	
					Longitudinal	Transverse
56	5	5	0.0292	10,300	40.5	35.0
57			.0370	10,300	42.2	36.5
58			.0483	10,300	46.5	39.0
59			.0530	10,300	44.0	38.0
60			.0641	10,300	43.2	38.0

TABLE 3.—RESULTS FOR PLATES WITH CLAMPED EDGES

Plate	Relative deviation, $\triangle w_0/w_{00}$ [a]	Navy yield pressure, p_y (lb/sq in.)	Pressure for span/500, $p_{2a/500}$ (lb/sq in.)	Pressure for span/200, $p_{2a/200}$ (lb/sq in.)
1	−0.84 a	74	45	78.5
2	−.30 a	71	38	65
3	−.08 b	27	19	29
4	.17 b	24.5	16.5	25.5
5	−.08 b	15	7.6	16.5
6	−.64 a	89	37	67
7	.10 b	50	23	45
8	.01 b	33	22	34
9	.09 a	31.5	42	66
10	−.46 b	57.5	31	53
10a	−.21 b			
11	−.08 b	37	25	39
12	−.28 b	11 to 27.5	14	22
13	.37 a	42	53	83
14	−.07 b	32 to 72	26	58
15	−.12 b	50	24	42
16	.36 a	50	63	90
17	.39 b	22.5	17	27
18	1.92 f	37.7	30	48
19	−.09 b	18.3	18.5	30
20	−.08 f	12 to 23	13	25.5
21	−.57 f	7 to 20	13.5	24.5
22	.39 a	87.5	93	130
23	.15 a	19.5	14	30
24	.80 g	55.8	42.5	60
25	.11 b	21	19	30
26	−.18 f	5 to 15	10.5	21.5
27	.68 b	155	145	192
28	.37 b	25	29	42
29	.21 b	16	18	24
30	−.11 f	5 to 15	10	20
31	.44 b	42	45	60
32	.09 b	20	21	29
33	.69 f	4 to 11	9.5	17
34	.23 b	62	67	84
35	.26 b	24.6	28.4	36.5
36	.30 f	8.4	13	23
37	.10 f	10 to 20	19	25
38	.41 b	140	130	175
39	−.06 b	28	40	78
40	−.23 b	18	19	27
41	.46 b	27	20	34
42	.86 b	92	86	165
43	−.25 b	13	21	33
44	1.24 g	34	34	44
45	.94 d	135	145	228
46	.34 b	24	28	40
47	1.07 g	46	48	61
48	1.06 e	188	260	430
49	.00 c	82	84	132
50	1.70 g	104	138	188
51	.04 f	52	28	55
52	.84 f	50	26	58
53	.94 f	58	56	79
54	−.01 f	35	25	48
55	.39 f	55	28	64

Letter	Value of w_{00} for p (lb/sq in.)	Reference
b	1	13
c	2	13
d	4	13
e	20	13
f	1	12
g	4	12

a, $w_{09}=h$, ref. 11.

TABLE 4.—RESULTS FOR PLATES WITH FREELY SUPPORTED EDGES

Plate	Relative deviation, $\triangle w_0/w_{00}$ [a]	Navy yield pressure, p_y (lb/sq in.)	Pressure for span/500, $p_{2a/500}$ (lb/sq in.)	Pressure for span/200, $p_{2a/200}$ (lb/sq in.)
56	−0.17 b	19.5	16	24
57	.00 c	24	20	28
58	−.20 d	44	37	51
59	−.18 a	47	40	58
60	−.03 a	55	53	67

Letter	Value of w_{00} for p (lb/sq in.)	Reference
a	1	8
b	$1<p<2$	8
c	$1<p<5$	8
d	$2<p<10$	8

U. S. GOVERNMENT PRINTING OFFICE: 1942

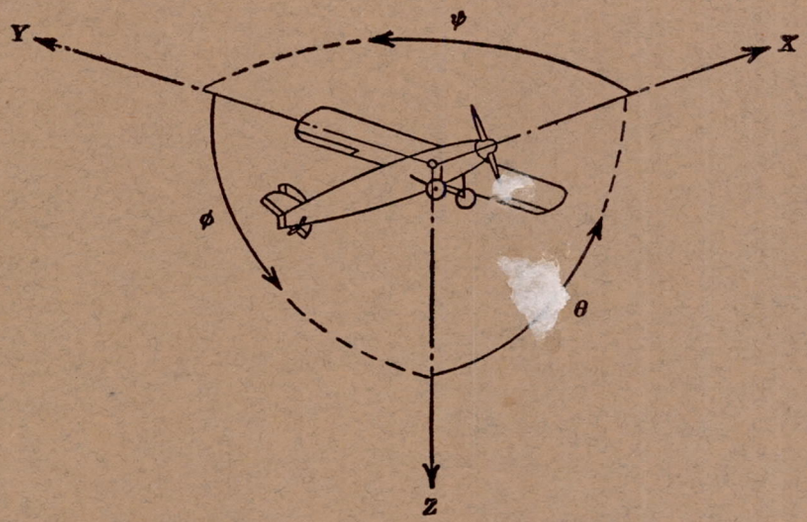

Positive directions of axes and angles (forces and moments) are shown by arrows

Axis		Force (parallel to axis) symbol	Moment about axis			Angle		Velocities	
Designation	Symbol		Designation	Symbol	Positive direction	Designation	Symbol	Linear (component along axis)	Angular
Longitudinal	X	X	Rolling	L	$Y \longrightarrow Z$	Roll	φ	u	p
Lateral	Y	Y	Pitching	M	$Z \longrightarrow X$	Pitch	θ	v	q
Normal	Z	Z	Yawing	N	$X \longrightarrow Y$	Yaw	ψ	w	r

Absolute coefficients of moment

$C_l = \frac{L}{qbS}$ (rolling) $\quad C_m = \frac{M}{qcS}$ (pitching) $\quad C_n = \frac{N}{qbS}$ (yawing)

Angle of set of control surface (relative to neutral position), δ. (Indicate surface by proper subscript.)

4. PROPELLER SYMBOLS

D Diameter

p Geometric pitch

p/D Pitch ratio

V' Inflow velocity

V_s Slipstream velocity

T Thrust, absolute coefficient $C_T = \frac{T}{\rho n^2 D^4}$

Q Torque, absolute coefficient $C_Q = \frac{Q}{\rho n^2 D^5}$

P Power, absolute coefficient $C_P = \frac{P}{\rho n^3 D^5}$

C_s Speed-power coefficient $= \sqrt[5]{\frac{\rho V^5}{P n^2}}$

η Efficiency

n Revolutions per second, rps

Φ Effective helix angle $= \tan^{-1}\left(\frac{V}{2\pi r n}\right)$

5. NUMERICAL RELATIONS

1 hp=76.04 kg-m/s=550 ft-lb/sec

1 metric horsepower=0.9863 hp

1 mph=0.4470 mps

1 mps=2.2369 mph

1 lb=0.4536 kg

1 kg=2.2046 lb

1 mi=1,609.35 m=5,280 ft

1 m=3.2808 ft